J Nanopart Res (2013) 15:2099
DOI 10.1007/s11051-013-2099-y

REVIEW

Graphene oxide-based drug delivery vehicles: functionalization, characterization, and cytotoxicity evaluation

Sami Makharza · Giuseppe Cirillo · Alicja Bachmatiuk · Imad Ibrahim · Nicholas Ioannides · Barbara Trzebicka · Silke Hampel · Mark H. Rümmeli

Received: 26 September 2013 / Accepted: 25 October 2013 / Published online: 12 November 2013

Abstract As a consequence of graphene oxides (GOs) high chemical versatility, there is great interest in functionalized as a nanocarrier for in vitro and in vivo drug delivery. Within this review, the structure and properties of GO that allow covalent and non-covalent functionalization are discussed. In short, toxicity investigations show functionalized GO is biocompatible. Various works demonstrate the potential of GO derivatives as exciting nanocarriers for the loading and delivery of therapeutic drugs.

Keywords Graphene oxide · Nanocarrier · Drug therapy · Health effects · Nanomedicine

Abbreviations

GO	Graphene oxide
NGO	Nanographene oxide
PEG	Polyethylene glycol
DOX	Doxorubicin
CPT	Camptothecin
MCF-7	Breast cancer cell line
CNT	Carbon nanotube
ND	Nanodiamond
AFM	Atomic force microscopy
FTIR	Fourier transform infrared spectroscopy
XPS	X-ray photoelectron spectroscopy

S. Makharza · G. Cirillo · I. Ibrahim · S. Hampel
IFW Dresden, 01171 Dresden, Germany

G. Cirillo
Department of Pharmacy, Health and Nutritional Sciences, University of Calabria,
87036 Arcavacata di Rende, CS, Italy

A. Bachmatiuk · M. H. Rümmeli
IBS Center for Integrated Nanostructure Physics, Institute for Basic Science (IBS), Taejon 305-701, Republic of Korea

A. Bachmatiuk · M. H. Rümmeli (✉)
Department of Energy Science, Department of Physics, Sungkyunkwan University, Suwon 440-746, Republic of Korea
e-mail: m.ruemmeli@ifw-dresden.de

A. Bachmatiuk · B. Trzebicka
Centre of Polymer and Carbon Materials, Polish Academy of Sciences, M. Curie-Sklodowskiej 34, Zabrze 41-819, Poland

N. Ioannides
Faculty of Life Sciences and Computing, London Metropolitan University,
166-220 Holloway Road, London N7 8DB, UK

CNMs	Carbon nanomaterials
SN38	7-Ethyl-10-hydroxycamptothecin
L-929	Murine fibroblast cells
PC12	Neuroendocrine cells
OLC	Oligodendroglia cells
OBS	Osteoblasts
hESc	Human embryonic stem cells
hFBc	Human fibroblast cells
hMSCs	Mesenchymal stem cells
LEc	Lung epithelial cells
A549	Adenocarcinomic human alveolar epithelial cells
FBS	Fetal bovine serum
EMT6	Mouse breast cancer cell line
ROS	Relative oxygen species
MTX	Methotrexate
MWCNT	Multiwall carbon nanotube

Introduction

Graphene has attracted significant interest in the areas of materials science, fundamental physics, and engineering since its discovery in 2004 (Novoselov et al. 2004, 2005). Owing to its unique two-dimensional structure and attractive physiochemical properties, graphene has been receiving exciting attention in many fields and primarily in those of biology and medicine. Graphene oxide (GO), a distinctive structure of sp^2 carbon, oxygen, and hydrogen in variable ratios, can be obtained by oxidizing graphite in an acidic medium (Hummers and Offeman 1958; Marcano et al. 2010). The presence of abundant functional groups (epoxy, hydroxyl, carboxylic groups), conjugation system, large surface area, low cytotoxic effect, and low cost (Liu et al. 2008; Sun et al. 2008; Zhang et al. 2010a, c, 2011a; Akhavan and Ghaderi 2010; Yang et al. 2011a, 2012c; Lee et al. 2011; Chang et al. 2011; Bao et al. 2011; Liao et al. 2011; Xiao and Chen 2012; Wang et al. 2012; Akhavan et al. 2012; Tang and Cao 2012; Chng and Pumera 2013) have led to a surge of important potential in drug loading and delivery. The functional groups, decorated the basal planes and edges of GO layers, significantly revise the van der Waals interactions between graphene sheets (Bourlinos et al. 2003; Scholz and Boehm 2004) and impart desirable dispersability in water and several organic solvents (Titelman et al. 2005; Paredes et al. 2008; Moazzami Gudarzi 2012). Moreover, these functional groups allow GO conjugation with polymers and drugs through both covalent and non-covalent modification techniques (Kuila et al. 2012). Furthermore, the high surface area and π-conjugated structure of GO enabled it, as a platform, to immobilize with a number of substances, including metallic nanoparticles, drugs, and fluorescent molecules for different applications (Lu et al. 2009; Zhang et al. 2010a; Liu et al. 2010; Loh et al. 2010b; Bao et al. 2011; Jayakumar et al. 2012; Kim et al. 2012; Wate et al. 2012). As a consequence of this high chemical versatility, several research groups have recently explored functionalized GO as a nanocarrier for in vitro and in vivo drug delivery. The continuously increasing research effort for GO-based drug delivery in the last decade is shown in Fig. 1.

The building of versatile drug carrier systems is considered a challenge on high capacity loading, efficient delivery, and specific targeting (Vashist et al. 2011; Liu et al. 2012; Szűts and Szabó-Révész 2012). Lui et al. focused on PEGylated nanographene oxide (NGO) for drug delivery of hydrophobic anticancer drug molecules via π–π stacking. Their results showed that NGO-functionalized polyethylene glycol (PEG) is biocompatible without evident toxicity (Liu et al. 2008). Zhang et al. synthesized GO-based folic acid-conjugated, in order to control co-loading of doxorubicin (DOX) and camptothecin (CPT). Their system shows specific cytotoxicity and targeting the breast cancer cell line Michigan Cancer Foundation-7 (MCF-7) (Zhang et al. 2010a). In addition, pristine

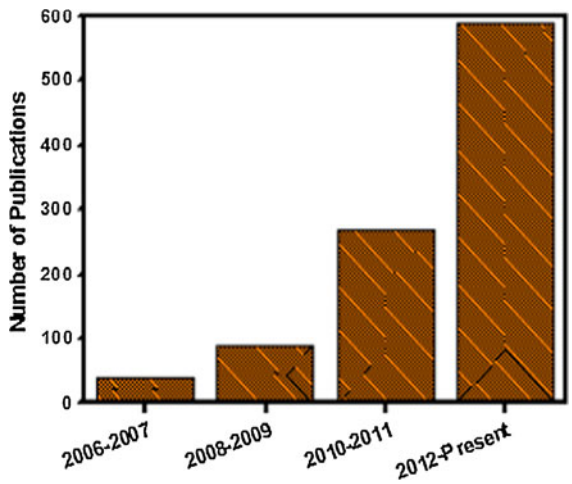

Fig. 1 Number of published articles in the last decade pertaining to GO-based drug delivery applications (based on data taken from www.sciencedirect.com on April 15, 2013)

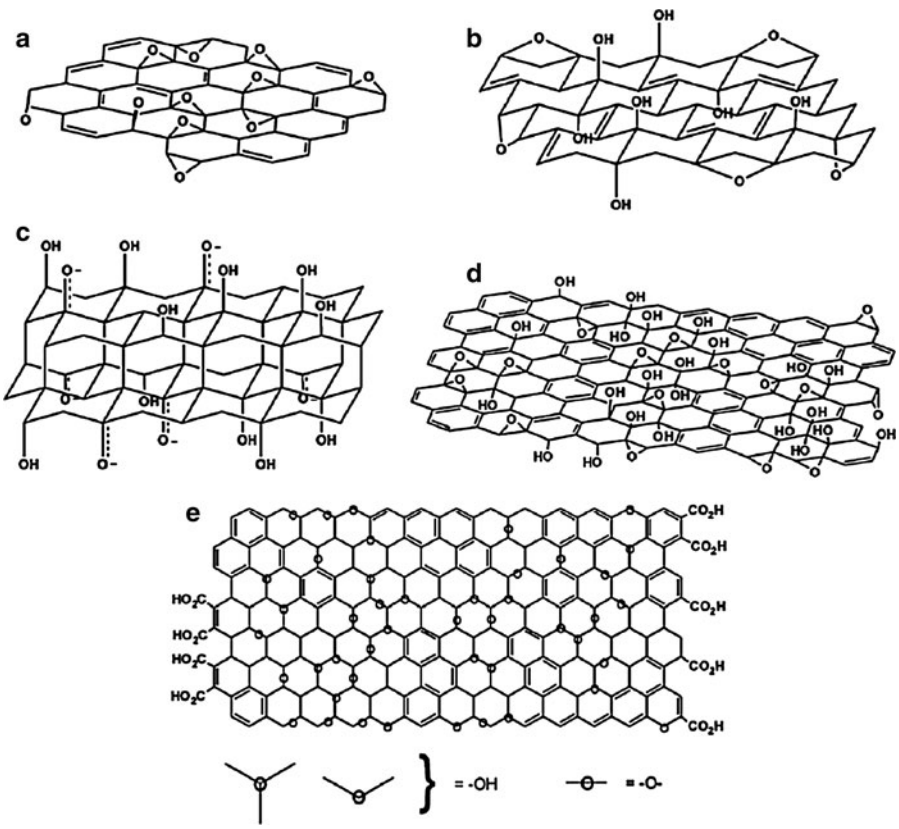

Fig. 2 Different model structures of GO: **a** Hofmann–Holst, **b** Ruess, **c** Nakajima–Matsuo, and **d**, **e** Lerf–Klinowski [deduced from Refs. (Lerf et al. 1998; Josepovits et al. 2006)]

graphene and GO have been investigated in vitro and in vivo in different cell types (Liao et al. 2011; Zhang et al. 2011b, 2012; Qin et al. 2012).

This review discusses and highlights the recent investigations of GO's applications in the field of drug delivery. The structure and properties of GO, covalent and non-covalent functionalization, characterization techniques, cytotoxicity of GO, and cytotoxicity of functionalized GO are also discussed. Later, GO-based drug delivery systems based on in vitro cellular uptake and in vivo cancer therapy are presented. Finally, a comparative study between carbon nanomaterials, such as carbon nanotube (CNTs), nanodiamond (ND), fullerene (C_{60}), and GO-based drug delivery systems is produced.

Graphene oxide

The structure and chemistry of GO have been discussed extensively in other reviews (Park and Ruoff 2009; Dreyer et al. 2010). The specific atomic structure of GO is not openly understood due to its random oxygen groups and irregular layer stacking. To this end substantial methods (models and experiments) have been developed toward understanding the GO structure. Hofman–Holst (2006), Ruess (Ruess 1946), and Nakajima–Matsuo (He et al. 1996) introduced model structures for GO. Lerf–Klinowski (Lerf et al. 1998) and Dekany (Buchsteiner et al. 2006) are the most well-known models using NMR to study the GO structure. Cai et al. (2008) used synthetic ^{13}C-labeled graphite for GO preparation. Their results revealed that the Lerf–Klinowski and Dekany models as the preferable structures for GO. Figure 2 illustrates different model structures of GO, showing the oxygen groups localized at the edges of graphene sheet as well as above and below the basal plane.

Structure and properties of GO

The chemical structure of graphene and GO is shown in Fig. 3. Over the years, considerable effort went toward understanding the structure of GO. In GO, the carbon atoms covalently bonded to oxygen containing groups are sp^3 hybrids and can disrupt the sp^2

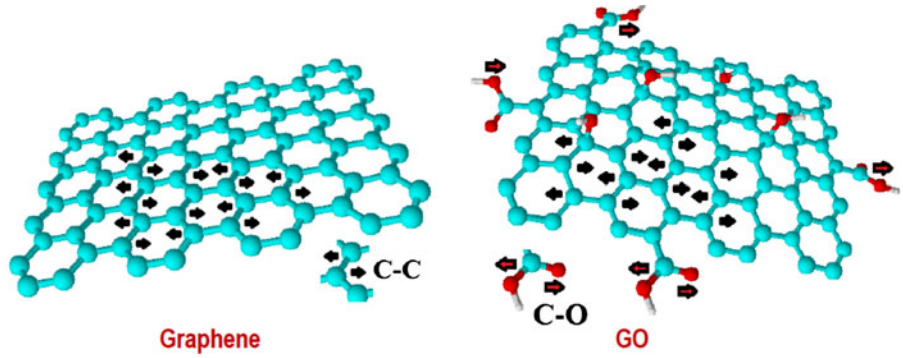

Fig. 3 Chemical structure of graphene and GO

conjugated system of graphene lattice structure (Gómez-Navarro et al. 2007; Eda et al. 2009). sp^3 hybridized regions are randomly distributed either in or out of the basal plane of graphene sheets or at the edges (Schniepp et al. 2006).

The properties of GO are unreliable and depend on its synthesis methods, processing, and experimental conditions. Electrically, GO is considered an insulating material due to its widespread saturated sp^3 bonds, vacancies (missing carbon atoms), and negatively charged density species bound to carbon. For these reasons, the energy gap increases and makes GO non-conducting (Boukhvalov and Katsnelson 2008; Jung et al. 2008b; Yan and Chou 2010). Nevertheless, the structural and electronic properties of GO can be modified via chemical and thermal treatments (Gilje et al. 2007; Becerril et al. 2008; Eda et al. 2008). The optical properties also depend on the oxidation level of GO (Jung et al. 2007, 2008c). The multiple layers of GO change considerably the corresponding optical properties, for instance, the refractive index of thermally reduced GO is higher than that in stacked GO. GO is highly soluble and disperses well in water and physiological media, making it attractive for medical purposes after numerous modifications.

Recently, in order to delve into the GO structure in more detail, several microscopic and spectroscopic methods have been employed to investigate the structure of GO and its chemical compositions, as will be shown later. Such methods include atomic force microscopy (AFM), scanning transmission electron microscopy (STEM) combined with electron energy loss spectroscopy (EELS), scanning tunneling microscopy (STM), high-resolution transmission electron microscopy (HRTEM), Raman spectroscopy, Fourier transform infrared spectroscopy (FTIR), and X-ray photoelectron spectroscopy (XPS).

In addition, theoretical studies have been considered for GO structural exploration, thus providing significant insight in its workable kinetic and thermodynamic structure. Depending on the first-principle calculations, the building blocks in GO (atomic energy configurations) have been identified as containing epoxy and hydroxyl groups close to each other (Yan and Chou 2010; Wang et al. 2010b; Lu et al. 2011; Yuan et al. 2011). Different arrangements of the building blocks have been found to yield a local density approximation band gap in the range of a few electron volts. This principle implies the possibility of opening and tuning the band gap of the GO depending on the degree of oxidation (Yan and Chou 2010; Yuan et al. 2011). Density functional theory (DFT) calculations revealed that the epoxy group is formed between the oxygen atom and two adjacent carbon atoms on the graphene network, while the hydroxyl group is formed on the opposite side (Lahaye et al. 2009). Furthermore, theoretical calculations have been used to study the atomic structure of reduced GO as well as the chemical changes of oxygen containing groups during reduction processes (Paci et al. 2007; Bagri et al. 2010; Acik et al. 2011; Larciprete et al. 2011).

Preparation protocols

The most common chemical routes for GO preparation begin from expandable graphite by chemical exfoliation using various oxidizing agents such as potassium permanganate ($KMnO_4$) and potassium chlorate ($KClO_3$). These routes were comprehensively covered in previous reviews (Park and Ruoff 2009; Dreyer et al.

2010) and are summarized in Table 1. The first procedures for GO were developed by Brodie (1859), Staudenmeier (1898), and Hummers and Offeman (1958). Brodie (1859) treated graphite with $KClO_3$ and fuming nitric acid (HNO_3). Staudenmaier (1898) improved Brodie's approach by slowly adding $KClO_3$ over 1 week to a solution containing concentrated sulfuric acid (H_2SO_4), concentrated HNO_3 (63 %), and graphite. The mass ratio of graphite to $KClO_3$ was 1:10. The possibility of explosion and length of time required are the main drawbacks of this approach. Hummers and Offeman (1958) reported an alternative method, which is safer and also not time consuming. In this protocol, a water-free mixture of concentrated H_2SO_4, sodium nitrate ($NaNO_3$), and $KMnO_4$ are involved; the reaction was performed at 45 °C and continued for approximately 2 h. Minor modifications to the Hummers method were developed and still remain in use (Kovtyukhova et al. 1999; Hirata et al. 2004).

Functionalization of graphene oxide

It is well known that carbon nanomaterials aggregate in cell culture media (buffers) caused by the charge screen effect. Therefore, surface modification is the key to render the solubility and the biocompatibility of carbon nanomaterials for biological systems. Depending on application purposes, two surface coating regimes are developed, including covalent and non-covalent approaches, allowing GO to be used in biological systems (Kitano et al. 2007; Bai et al. 2009; Veca et al. 2009; Yang et al. 2009c, 2012c; Choi et al. 2010; Widenkvist 2010; Englert et al. 2011). Before surface functionalization, the size distribution and individual separation of GO are essential for in vitro and in vivo drug delivery.

Covalent functionalization

The covalent functionalization of nanoscaled carbon nanomaterials (CNMs) is preceded by an oxidation of the graphite in acidic media with strong oxidizing agents, resulting in oxygen-rich groups. As described above, the GO is highly oxidized by oxygen groups with C/O ratio of 2:1. The presence of these functional groups allows various chemical routes already known in chemistry to functionalize GO (Fig. 4) (Loh et al.

Table 1 The oxidation methods of graphite to graphite oxide

	Brodie	Staudenmaier	Hummers & Offeman	Modified Hummers	
Year:	1859	1898	1958	1999	2004
Agents	$KClO_3$, HNO_3	$KClO_3$ (or $NaClO_3$), HNO_3, H_2SO_4	$NaNO_3$, $KMnO_4$, H_2SO_4	Pre-ox: $K_2S_2O_8$, P_2O_5, H_2SO_4 ox: $KMnO_4$, H_2SO_4	$NaNO_3$, $KMnO_4$, H_2SO_4
C:O ratio	2.16 (Brodie 1859)	N/A (Staudenmaier 1898)	2.25 (Hummers and Offeman 1958)	1.3 (Kovtyukhova et al. 1999)	1.8 (Hirata et al. 2004)
	2.28 (He et al. 1996)	1.85 (He et al. 1996)	2.17 (He et al. 1996)		
Reaction time	≈ 72 h (Brodie 1859)	24–48 h (Staudenmaier 1898)	≈ 2 h (Hummers and Offeman 1958)	6 h pre-ox + 2 h ox (Kovtyukhova et al. 1999)	≈5 days (Hirata et al. 2004)
	10 h (He et al. 1996)	10 days (He et al. 1996)	9–10 h (He et al. 1996)		
Intersheet spacing (Å)	5.95 (He et al. 1996)	6.23 (He et al. 1996)	6.67 (He et al. 1996)	6.9 (Kovtyukhova et al. 1999)	8.3 (Hirata et al. 2004)

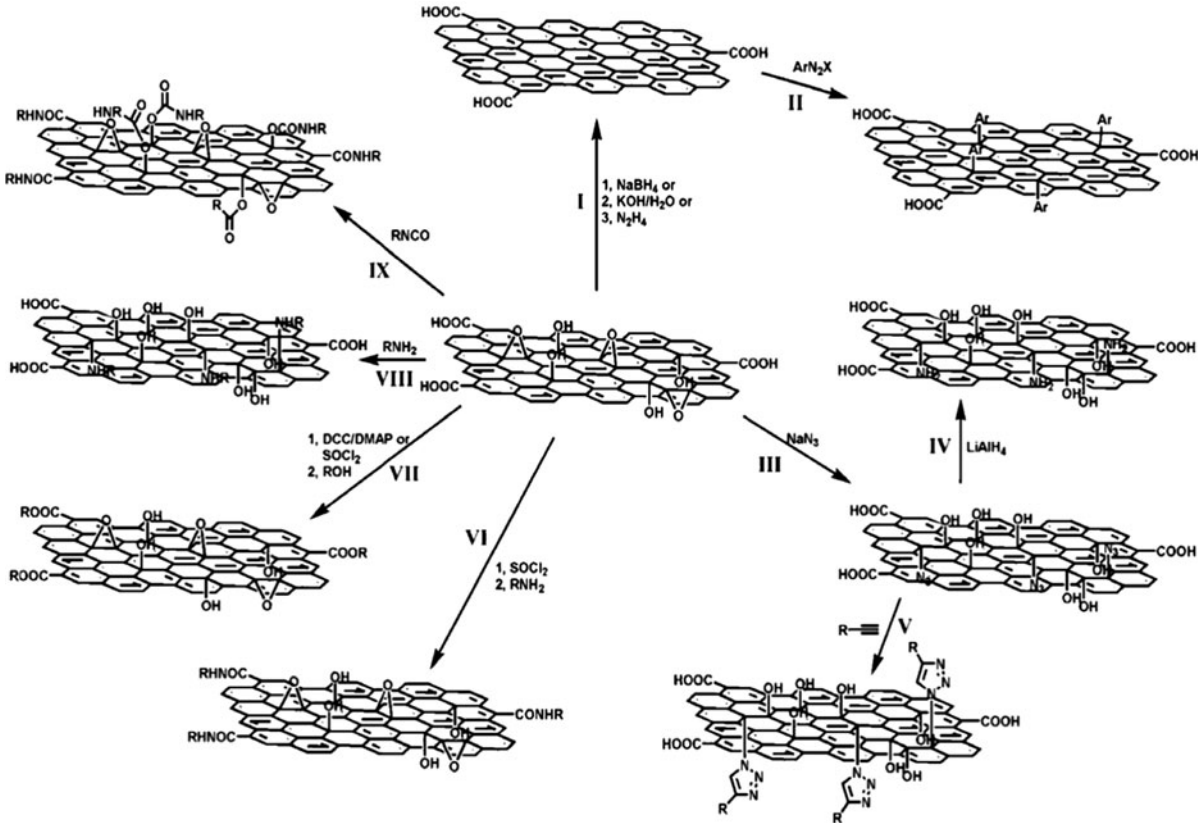

Fig. 4 Schematic illustration showing various covalent functionalizations of graphene or GO: *I* Reduction of GO [*1* $NaBH_4$, *2* KOH/H_2O, *3* N_2H_4]. *II* Covalent functionalization of reduced graphene via diazonium reaction (Si and Samulski 2008; Lomeda et al. 2008). *III* Functionalization of GO by the sodium azide. *IV* Reduction of azide-functionalized GO with $LiAlH_4$ producing amino-functionalized GO. *V* Functionalization of azide–GO through (R–ChCH/$CuSO_4$). *VI* Modification of GO with the acylation reaction. *VII* Esterification of GO by activation of the COOH groups (*1* DCC/DMAP or $SOCl_2$, *2* ROH). *VIII* Nucleophilic ring-opening reaction. *IX* Covalent functionalization of graphene oxide via organic isocyanates. Reproduced with permission from Marques et al. (2011)

2010a). The acylation reactions are the most common routes used for binding molecular moieties onto oxygen-rich groups at the edges of GO. Carboxylic acid groups at the edges have the ability to bind with octadecylamine to modify GO by long alkyl chains (reaction VI in Fig. 4) that can be tethered to amine-functionalized molecules (Xu et al. 2009). Depending on this covalent functionalization, NGO-functionalized PEG is used to obtain a biocompatible conjugation system which can be performed as a platform for drug delivery (Sun et al. 2008). It is known that aromatic drug molecule 7-ethyl-10-hydroxycamptothecin (SN38) is water insoluble and hard to be used for the treatment of diseases. The resulting NGO–PEG/SN38 conjugation exhibits high water solubility while retaining a high cancer cell therapy similar to that of the free drug in organic solvents. The water soluble SN38 prodrug has been investigated in colon cancer treatment (Liu et al. 2008). The epoxy groups can undergo nucleophilic ring-opening reaction with amine-terminated molecules (reaction VIII in Fig. 4). For instance, octadecylamine (Wang et al. 2008), 1-(3-aminopropyl)-3-methylimidazolium bromide (Yang et al. 2009c), and 3-aminopropyltriethoxysilane (Lin et al. 2011; Wang et al. 2011) have been reacted with epoxy groups on the GO surface and afforded colloidal suspensions of GO in various polar solvents, such as water, DMF, and DMSO (Wang et al. 2008; Sun et al. 2010). The resultant amine-functionalized GO has been used in various applications, such as

optoelectronic (Xu et al. 2009), biodevices (Mohanty and Berry 2008), polymer composite (Veca et al. 2009), and drug delivery (Liu et al. 2008).

Non-covalent functionalization

Non-covalent functionalization with different chemical substances is essential and considered to have less impact on the structure and properties of graphene. The attachment of functional groups to GO occurs via π–π, electrostatic binding, H-bonding, van der Waals, H–π, cation–π, and anion–π interactions (Tarakeshwar et al. 2001; Grimme 2004; Yi et al. 2006, 2009; Lee et al. 2007; Singh et al. 2009; Riley et al. 2010; Ma and Dougherty 2012). The π–π interaction is one of the most interesting non-covalent interactions; the diffuse electron clouds in the π systems exhibit attractive forces. For sufficient stability in aqueous solutions, graphene and GO via non-covalent interaction usually occur with surfactant molecules or amphiphilic polymers. However, biocompatible polymers for RGO surface coating are more useful than small surfactant molecules (Park et al. 2010). For the first time, via non-covalent functionalization, PEGylated NGO were employed as a nanocarrier to load therapeutic anticancer drugs and its cellular uptake was studied (Liu et al. 2008; Sun et al. 2008). Hu et al. developed graphene–pluronic F127 (PF 127) nanohybrid, the hydrophobic moieties of PF 127 attached to graphene surface via hydrophobic binding and the hydrophilic chains of PF 127 remained free to move in solution (Hu et al. 2012). PEG-grafted poly(maleic anhydride-alt-1-octadecene) via non-covalent produced sufficient physiological stability and increases blood circulation half-life in photothermal cancer therapy (Yang et al. 2012a, b). GO sheets possessed high negative charge; positively charged molecules could bind via electrostatic interactions. Liu et al. used polyethyleneimine (PEI) as cationic polymer to non-covalent coat GO and the results showed that the obtained GO-PEI has improved stability in culture media, high gene transfection efficiency, as well as reduced toxicity against treated cells (Feng et al. 2011). Tan et al. introduced L-proline/GO hybrid through hydrogen bonding interaction; the result revealed that the loading of L-proline onto GO (Fig. 7d) is highly efficient in hybrid catalysts compared with unloaded L-proline for the direct asymmetric aldol reaction (Tan et al. 2013a).

In a nanocarrier system, Depan et al. used positively charged polymer to encapsulate DOX-loaded GO, obtaining DOX–GO–chitosan–folate nanocarrier system that exhibited a pH response drug release profile (Depan et al. 2011). Protein-coated GO, demonstrated in many reports (Liu et al. 2011; Hu et al. 2011; Shen et al. 2012; Tan et al. 2013b), sonication of fetal bovine serum non-covalent-functionalized GO exhibits low cytotoxicity compared with uncoated GO (Hu et al. 2011). Owing to their high conjugation system (π–π delocalization regime), pristine graphene and GO possess the ability to bind with aromatic compounds through π–π stacking, including cancer drugs, fluorescence molecule (fluorescein), catalytic hybrid, and combinations of molecules.

Characterization techniques

A variety of characterization techniques have been used to utilize the structure and properties of GO. These techniques are classified into spectroscopic and microscopic approaches. The spectroscopic approaches are used to identify the chemical structure of GO, and include Raman, FTIR, and XPS. Microscopic tools are used to map out the structure of GO at various heights and lateral dimensions. For instance, AFM, SEM, TEM, and STM (Kovtyukhova et al. 1999; Sun et al. 2008; 2010; Lomeda et al. 2008; Loh et al. 2010b; Englert et al. 2011; Han et al. 2011; Du et al. 2011; Chang et al. 2011; Xiao and Chen 2012; Cheng et al. 2013).

Spectroscopic approaches

Raman spectroscopy

Raman spectroscopy, introduced by Krishna and Raman in 1981 (Rousseau et al. 1981), is a spectroscopic technique that provides information about molecular vibrations and can be used for sample identification and quantification. It is based on Raman scattering when monochromatic light hits a sample. The Raman effect occurs when light impinges upon a molecule and interacts with the electrons that bond to that molecule. As a result, a photon excites the molecule from the ground state to a virtual energy state. Later, the molecule returns back to a different rotational or vibrational state emitting a photon in the process. A detector detects the energy of the

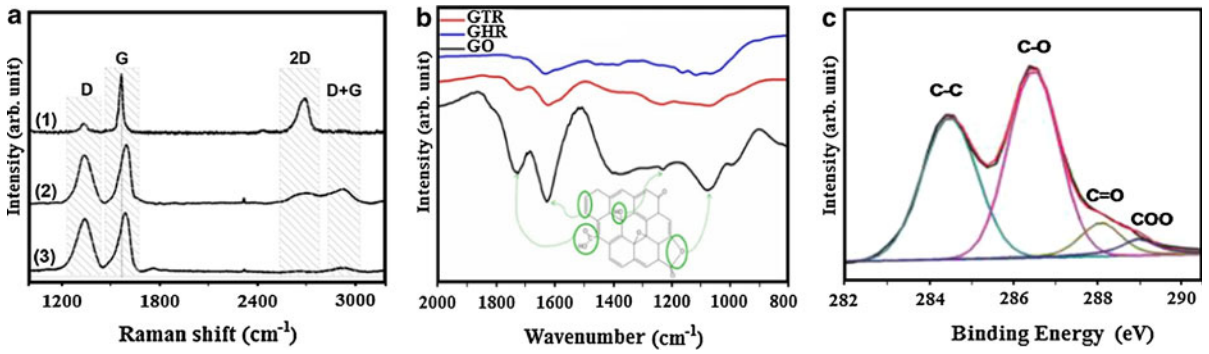

Fig. 5 Typical spectra for the GO as gathered by **a** Raman spectroscopy (Makharza et al. 2013), **b** FTIR (Marques et al. 2011), and **c** XPS (Xue et al. 2012)

released photon which equals to the energy difference between the original state and the new molecule state. This energy difference leads to an up or down shift in the emitted photon's frequency away from the excitation wavelength frequency. Raman shifts can provide information about vibrational, rotational, and other low frequency changes in the samples (Dresselhaus et al. 2004; Ferrari and Robertson 2004; Reich and Thomsen 2004).

Raman scattering is a powerful characterization technique used as a probe of order and disorder in the carbon skeleton of sp^2 and sp^3 hybridized carbon-based materials. Graphite material (multiple graphene sheets) has three dominant Raman features at $\sim$1,580 cm^{-1} (G bank), $\sim$1,350 cm^{-1} (D band), and $\sim$2,700 cm^{-1} (2D band) as shown in a of Fig. 5. The G mode corresponds to planar vibrations of carbon atoms and is present in most graphite-like materials. The D mode is related to the structural defects and is present in all graphite-like carbon materials. A weak band at $\sim$3,248 cm^{-1} (2D′ band) corresponds to an overtone of D′ (1,620 cm^{-1}) mode (Das et al. 2008). One layer of highly crystalline graphene sheet has a 2D mode at lower frequency in comparison with graphite, the width of this band being around 24 cm^{-1} for monolayer graphene and varies for graphite from 45 to 60 cm^{-1}. Moreover, the relative intensity of 2D and G bands—I_{2D}/I_G in monolayer graphene sheet is higher than in graphite (Pimenta et al. 2007; Cançado et al. 2008; Malard et al. 2009). In GO, the G band is wider and shifted to a lower frequency region ca. 1,590 cm^{-1}, the D mode intensity increases and probably becomes higher than the G mode due to the structural disorder in the sp^2 pattern induced by oxygen containing groups on the carbon basal plane or at the edges. On the other hand, the 2D mode reduces and becomes wider with respect to the D and G bands (Kudin et al. 2008; Yang et al. 2009a; Wilson et al. 2009). Typical Raman spectra of GO are shown in Fig. 5a. Raman spectroscopy bands D, G, and 2D might give insight after graphene or GO functionalization; Zhong et al. functionalized graphene with Aryne molecules, the results showing the I_D/I_G ratio of the functionalized graphene increasing for all Arynes after covalent functionalization (Zhong et al. 2010). Further functionalization of GO shows no significant changes when characterizing with Raman spectroscopy (Pasricha et al. 2009; Zhang and Zhang 2011).

Fourier transform infrared spectroscopy (FTIR)

Another spectroscopy technique yielding complementary information to those provided by Raman spectroscopy is infrared spectroscopy (IR). It excites a sample under observation with light in the infrared region of the electromagnetic spectrum. The infrared portion of the electromagnetic spectrum is divided into three regions: the near-, the mid- and the far-infrared. The mid-infrared is usually used to study the fundamental vibrations and associated rotational–vibrational structure, and the most related to the study of GO, as it contains the most useful vibrational frequencies of various oxygen groups. IR is based on the fact that the molecules absorb specific frequencies which match the frequency of the bond or group that vibrates. Radiation in the IR range is passed through the sample under investigation while the absorption coefficient of each wavelength is measured. The absorption of the radiation depends on the vibrational modes in the sample structure. Hence, each structure,

depending on the existing vibrational modes, has its characteristic absorption spectrum (fingerprints). Consequently, the IR spectrum is frequently used in order to identify the presence or absence of specific functional groups in a molecule. In the case of GO, the most characteristic peaks are the broad peak of hydroxyl group (–OH) at 3,430 cm^{-1}, the peak at 1,720 cm^{-1} corresponding to carbonyl group (C=O), 1,570 cm^{-1} representing the skeletal vibrations of sp^2 carbon atoms, 1,225 cm^{-1} and ca. 1,100 cm^{-1} referring to stretching vibrations of COOH and C–O–C, respectively (Fig. 5b) (Stankovich et al. 2006; Xu et al. 2009; Yang et al. 2011b; Acik et al. 2011).

X-ray photoelectron spectroscopy (XPS)

XPS, also called electron spectroscopy for chemical analysis (ESCA), is a quantitative spectroscopic technique that utilizes photo-ionization and analysis of the kinetic energy distribution of the emitted photoelectrons in order to study the elemental composition, empirical formula, chemical state, and electronic state of the elements that exist within a material. XPS spectra are created by irradiating a material with a beam of X-rays in ultra-high vacuum (UHV) conditions, forcing the core electrons to be excited into unoccupied atomic/molecular orbitals above the Fermi level. Simultaneously, the kinetic energy in addition to the number of electrons that escape from the top few nanometer of the material being analyzed is measured.

This technique is particularly useful for identification of carbon nanomaterials, in which the chemical composition greatly influences their properties. High-resolution XPS survey scan provides information not only about the identity of elements, but also the ratios of these elements detected. In addition, it provides insight into the identity of the functional groups distributed onto the surface which modulate the carbon nanomaterial's properties. For instance, XPS spectra of graphite have a strong peak, corresponding to C–C sp^2 at 284.5 eV, and small one at 289 eV from plasmons (Briggs and Seah 1990; Vickerman 1997), which represent collective behavior of the delocalized electrons. In GO, XPS further unambiguously exhibits the carbon and oxygen bonds in their various forms; C–C (sp^2 or sp^3), C–OH, C–O–C, C=O, and C=OOH. The C1's signal of these functional groups reveals at 284.5, 285.8, 286.5, 287.5, and 289.2 eV, respectively (Yang et al. 2009a; Mattevi et al. 2009; Lee et al. 2009; Akhavan 2010; Ganguly et al. 2011), as shown in c of Fig. 5. O1s provide complementary information to those in the C1s spectra, the deconvolution of O1s produces three main peaks around 531.1, 532.4, and 533.4 eV which are ascribed to C=O (oxygen atom connected to aromatic carbon), C–O (oxygen atom connected to aliphatic carbon), and C–OH (oxygen atom connected to aromatic carbon to form phenolic groups), respectively (Schniepp et al. 2006; Stankovich et al. 2007; Mattevi et al. 2009; Bagri et al. 2010). Intercalated adsorbed water molecules appeared at higher binding energy (534.7 eV) (Akhavan 2010). Moreover, XPS provides information about the identity of different kinds of metal ions like K, Na, Cu, Ni, Co, Cu, Ag, Mg, Pt, etc., as well as information on the valences and the ratio of these metals (Marcus and Maurice 2006; Stankovich et al. 2007; Altavilla and Ciliberto 2010).

Microscopic approaches

Microscopes have been important instruments for nano-structured materials. Various techniques are being used to understand the surface features of nanomaterials, such as optical microscopy, AFM, scanning electron microscopy, and high-resolution transmission electron spectroscopy.

Optical microscopy

For general evaluation of graphene and GO sheets, optical microscopy remains essential, a high throughput, and low cost imaging tool. Relatively, single-graphene sheet absorbs 2.3 % of the visible light (Nair et al. 2008; Duong et al. 2012). Reflected light microscope can provide high contrast images of graphene and GO (Novoselov et al. 2005). This allows researchers to scan the surfaces rapidly and measure the distribution and the shape of the GO flakes (Novoselov et al. 2004), as shown by the typical representative optical image in Fig. 6a.

Atomic force microscopy (AFM)

AFM is a high-resolution type of scanning probe microscopy. It is a method to visualize the surface topology of materials in three-dimensional (3D) detail down to the nanometer scale (Haugstad 2012). AFM

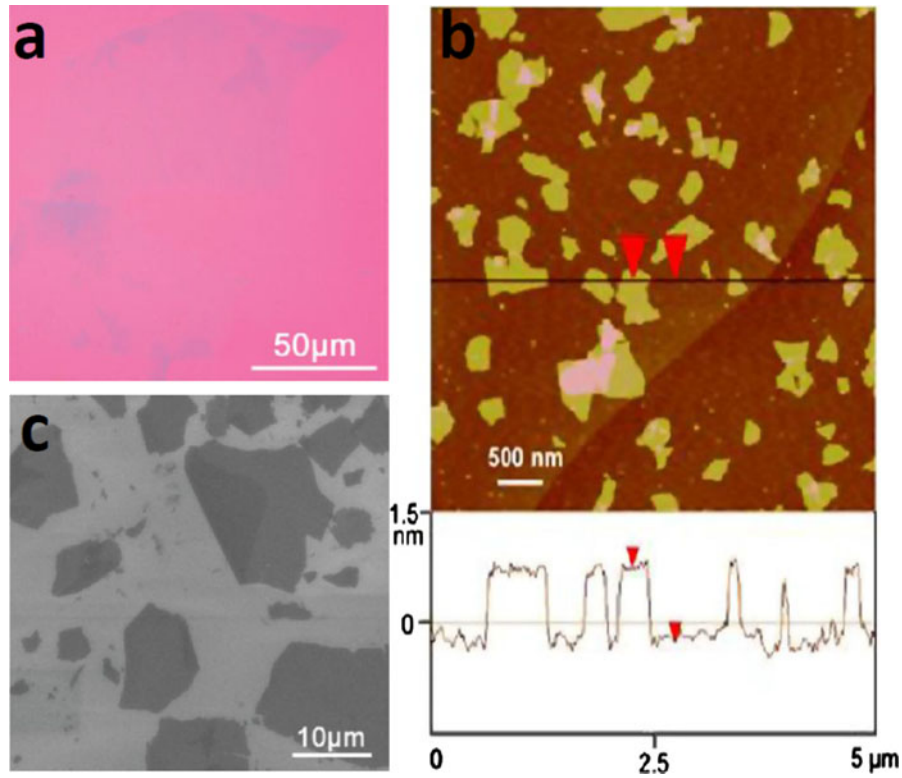

Fig. 6 Representative microscopy characterization of GO with **a** optical microscopy (Zhao et al. 2010), **b** AFM (Zhang et al. 2011c), and **c** SEM (Zhao et al. 2010)

reveals the thickness of graphene and GO sheets, as well as the number of layers (Stankovich et al. 2007; Gómez-Navarro et al. 2007; Cote et al. 2009; Paredes et al. 2009; Cheng et al. 2013). Moreover, it can show the distance between two graphene or GO layers which is essential to distinguish between them. The topological information of the surface is gathered by "feeling" the surface with a mechanical probe (tip) fixed on a cantilever. This mechanical probe (tip) scans the measured surface in a raster scan manner, while the van der Waals forces determine the deflection of the cantilever. Piezoelectric elements that facilitate tiny, accurate, and precise movements control the probe motion. AFM uses a laser beam detection system in order to control the piezoelectric element movements, where the laser is reflected from the back of the deflected cantilever onto a position-sensitive detector. AFM works in three main modes: tapping mode, contact mode, and non-contact mode AFM (Warner et al. 2012). Tapping mode is frequently used in characterizing GO as it allows high-resolution imaging without inducing destructive frictional forces onto the sample under investigation (Zhong et al. 1993).

In GO, due to the presence of oxygen groups, the interlayer distance between GO sheets increased to 0.7 nm, which is roughly twice the distance found in bilayer graphene sheets (Fig. 6b). Thus, the expected height measurements by AFM might exceed that of graphene. Shen et al. (2009) investigated the thickness of individual GO and reduced GO nanoplatelets. The results showed the average thickness of an exfoliated GO nanoplatelets is ca. 1.3 nm while the reduced GO sheets exhibited a bumpy structure with flat areas showing heights of 0.2–0.4 nm and some high areas manifested an average height of 1.5 nm. The bumpy regions attributed to the dead space due to vast edge functionalization (Dideykin et al. 2011). GO-based polymer functionalization showed an increase in the height more than that of pristine GO (Layek et al. 2010). The average thickness of graphene-functionalized polymer (methyl methacrylate—MMA) is 3 nm (Fang et al. 2009). Two different sites of functionalization (edge and graphene basal planes) are mostly responsible for height distributions. NGO–PEG/DOX drug loading produced an obvious increase in thickness compared with the precursor NGO (Sun et al. 2008). The same results deduced after loading of CPT

and SN38 onto NGO–PEG as a nanocarrier for drug delivery systems (Liu et al. 2008).

Scanning electron microscopy (SEM)

SEM is one of the most frequently used techniques in sample characterization, due to its good resolution, ease of applicability, large depth of focus, and high magnification. It is a type of electron microscope which images a sample by raster scanning it with a focussed beam of high-energy electrons. In a typical setup, an electron gun emits a high-energy electron beam in a high vacuum chamber, which later passes through a series of focussing and accelerating magnetic lenses. The high kinetic energy, carried by the accelerated electrons, is dissipated as a variety of signals produced by electron–sample interactions when the incident electrons are decelerated in the solid sample, including, in addition to many, the secondary electrons. The generated signals are then drawn to the secondary electron detector which is highly positively charged and guided through the Faraday cage to the collection target. Finally, they are converted into 2D grayscale images.

SEM is a versatile method used to gain information on the graphene and GO domains like size, shape, and nucleation density (Fig. 6c). It has also, recently, been used to study monolayer graphene onto different surfaces (Kim et al. 2009; Wood et al. 2011; Takahashi et al. 2012).

Cytotoxicity of graphene oxide

Graphene paper has been developed to be a biocompatible platform for adhesion and proliferation of murine fibroblast cells (L-929) (Chen et al. 2008), neuroendocrine cells (PC12), oligodendroglia cells (OLC), and osteoblasts (OBS) (Agarwal et al. 2010). Recently, in vivo cancer treatment using graphene as nanocarrier has been performed in animal experiments (Yang et al. 2010, 2011a). Various cytotoxicity investigations have been evaluated on graphene, GO, and functionalized GO in different cell lines (Zhang et al. 2010c, 2012; Wang et al. 2010a; Chang et al. 2011; Hu et al. 2011; Liao et al. 2011; Yang et al. 2012c). GO is a highly biocompatible material, thus, it inspirits the proliferation and adhesion of kidney cells, OBS, and human embryonic stem cells (hESc) (Agarwal et al. 2010; Park et al. 2010). On the contrary, other studies showed GO nanosheets mixed to cell culture media at 20 μg/mL can produce 20 % reduction in cell viability, whereas 50 μg/mL GO induce 50 % loss in cell viability. This result was attributed to inhibitory effect due to the GO suspension (Hu et al. 2010). Wang et al. examined human fibroblast cells (hFBc) with GO at different concentrations and found that concentration dependent on cytotoxicity when the concentration exceed 50 μg/mL (Wang et al. 2010a). For the first time, the cyto- and geno-toxic effect of reduced GO nanoparticles were investigated with mesenchymal stem cells (hMSCs) (Akhavan et al. 2012), with the study showing that the size and the concentration of GO are effective parameters on the hMSCs cytotoxicity.

Among these contradictory findings, there is no consensus on the cellular toxicity of GO, with different studies showing different biocompatibility of GO. For this inconsistency, Pumera and Chng reported the toxicity of GO depending on the oxidative methods used. They prepared GO by four different preparation methods (Staudenmaier—ST, Hofmann—HO, Hummers—HU, and Tour—TO), and investigated GO in adherent lung epithelial cells (LEc) by using in vitro MTT and WST-8 viability assays. The results revealed that different oxidizing methods exhibited different toxicological behavior of GOs as they contain different oxygen-based groups. All four GO nanomaterials', GO-ST, GO-HO, GO-HU, and GO-TO, exposure with adenocarcinomic human alveolar epithelial cells (A549) media are dose-dependent cytotoxic responses. Varieties of oxygen groups and (C/O ratio) play an important role in the toxicity of GO nanoplatelets (Chng and Pumera 2013). It is generally agreed that the oxygen groups, preparation methods of GO, size, charge, and the structural defects of graphene might disturb its in vivo and in vitro behavior and its toxicity in biological applications.

Cytotoxicity of functionalized GO

As previously discussed, GO needs to be functionalized in order to perfectly disperse in culture media, as well as being compatible with tissue organisms. Indeed, GO revealed two types of functionalization (covalent and/or non-covalent) with small molecules or macromolecules, depending on the chemical structure of materials used for GO modification. The

toxicity of pristine graphene and GO to mice are dose-dependent (Wang et al. 2010a; Yan et al. 2011; Zhang et al. 2011c). Functionalized NGO with biocompatible materials such as PEG (Sun et al. 2008; Yang et al. 2011a), dextran (Zhang et al. 2011a), chitosan (Fan et al. 2010; Liao et al. 2011), pluronic (Duch et al. 2011), tween (Park et al. 2010), low generation polyamidoamide (PAMAM) (G0) dendrimer (reference—our previous work), polyvinylpyrrolidone (PVP) (Qin et al. 2012), gelatin (An et al. 2013), sulfonic acid groups (Zhang et al. 2010a), and protein (fetal bovine serum—FBS) (Hu et al. 2011), show high reduction in vitro and in vivo toxicity. In the same context, Zhang et al. measured the cell viability percent of NGO–PEG vehicles as a function of concentration (Zhang et al. 2011b), and the data showed that above 95 % of mouse breast cancer cell line (EMT6) remained viable even at high concentration up to 100 μg/mL, which revealed that NGO–PEG has no cytotoxic effect to EMT6 cells after 24 h incubation. In other studies, gelatin-functionalized graphene nanosheets exhibited very low cytotoxic effect against A549, even at high concentration (300 μg/mL).

Surface modification of GO with appropriate biocompatible materials increases the uptake impact on various cell lines and retorts on the negative performance of pristine graphene and GO via a number of mechanisms such as relative oxygen species (ROS) and cell wall membrane damage.

Loading and delivery of drugs

In vitro tests

The large surface area of graphene makes it a strong candidate for drug loading other than commonly used carbon nanomaterials. It has a significant capability to interact with aromatic anticancer drugs and water insoluble drug molecules via strong π–π interaction (Sun et al. 2008; Liu et al. 2008). Doxorubicin (DOX) and water insoluble SN38 are the first two drug molecules loaded on PEGylated (PEG) nanographene oxide (NGO–PEG) (Fig. 7a). DOX loading onto NGO–PEG achieved by simple mixing of 0.5 mmol/L with NGO–PEG solution ($\sim$0.2 mg/mL) at pH 8 overnight via physisorption π stacking. NGO–PEG–Rituxan/DOX with Raji B—cells investigated in vitro (Fig. 7b), the result revealed that DOX delivery into Raji B—cells enhanced in NGO–PEG–Rituxan/DOX comparing with free DOX, NGO–PEG/DOX. Thiolated Rituxan (CD20 + antibody) conjugated to the amine groups onto NGO–PEG is used for selective killing of cancer cells (Sun et al. 2008). Also in this study, approximately 40 % of DOX released after 24 h in acidic solution (pH 5.5), this value of pH ascribed to increase the solubility and hydrophilicity of DOX for drug delivery analog, as well as accelerate the drug releasing (Fig. 7c). Zhang et al. found over 68 % of DOX released after 7 days at pH 5.5 (Zhang et al. 2011b). The pH of the medium is crucial in controlled drug delivery applications, for instance, extracellular tissues of cancer cells. In addition to the intracellular lysosomes and endosomes are acidic (Gillies and Fréchet 2005), which will drive the drug to be released from NGO–PEG structure. The loading quantity of DOX onto NGO–PEG was calculated to be 142.5 wt%, this amount of loading is higher than that in common drug delivery materials (Murakami et al. 2004; Liu et al. 2007b) which is always less than 100 %.

The drug model (methotrexate—MTX) loaded on gelatin–GNP showed that pH-dependent release at low pH was better than in neutral conditions (An et al. 2013). MTX@gelatin–GNP showed lower cytotoxic effect with A549 cells in comparison with free MTX at the same concentration. Water insoluble molecule SN38 loaded NGO–PEG via π–π stacking revealed excellent solubility in the biological environment (Liu et al. 2008), NGO–PEG/SN38 exhibited high influence to kill cancer cells in vitro, with a human colon cancer cell line (HCT-16). Folic acid-loaded NGO with the two anticancer therapeutic drugs (DOX and CPT-11) showed specific targeting to MCF-7 human breast cancer cells, as well as high cytotoxicity compared to unmodified NGO loaded with DOX or CPT.

In vivo tests

The in vivo therapeutic efficacy of NGO–PEG/DOX was demonstrated through combination of photothermal treatment and chemotherapy (Zhang et al. 2011b). As shown in Fig. 8a, four mice groups were treated with PBS (200 μL), DOX (10 mg/kg, 200 μL), NGO–

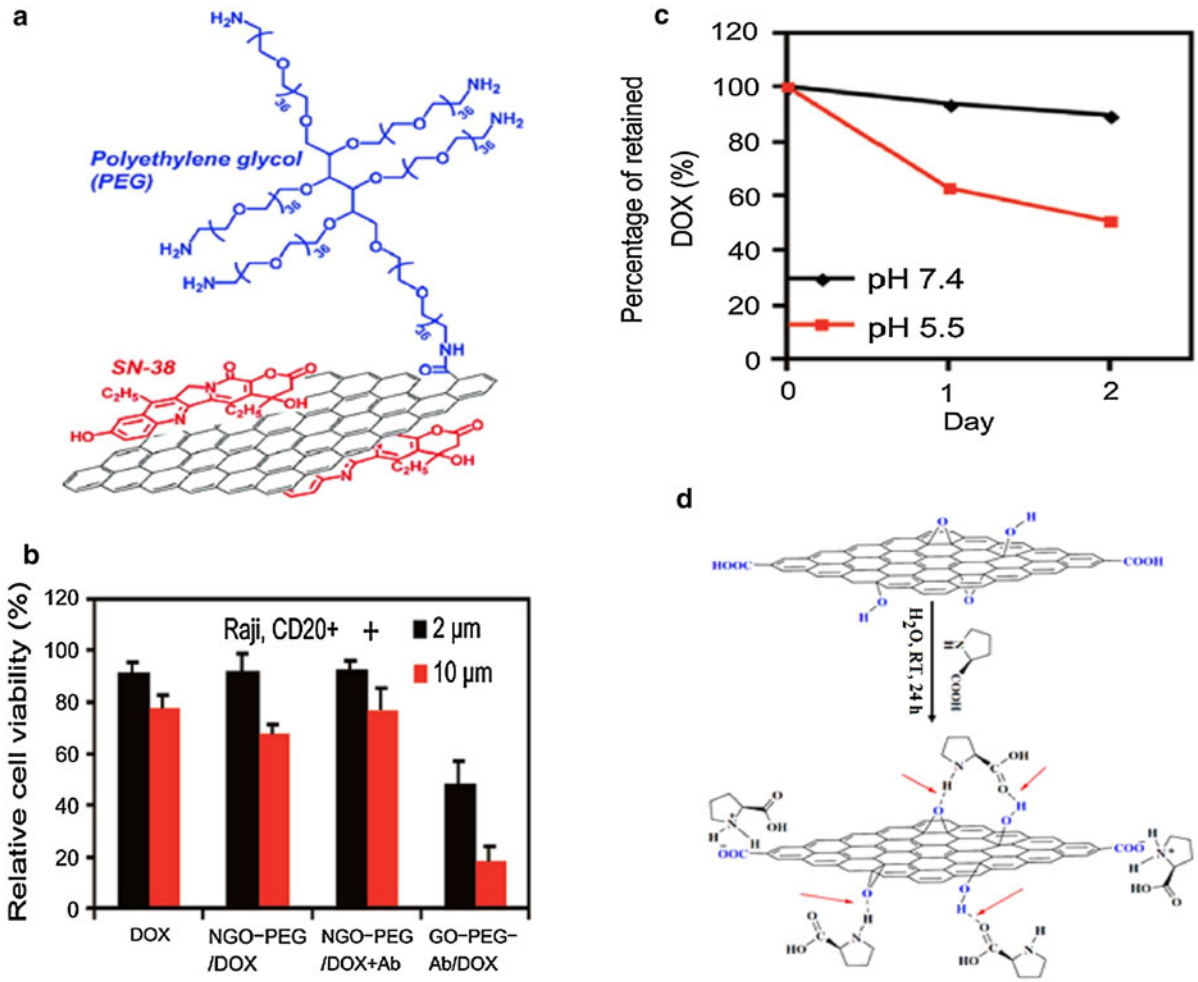

Fig. 7 **a** A schematic illustration of a 6-arm branched PEG covalently bound to GO and SN 38 loading onto NGO–PEG via π–π stacking. **b** Relative cell viability of free and conjugated DOX at 2 and 10 μM concentrations via MTS assay. **c** Percentage of DOX retained versus time onto NGO–PEG in PBS solution at pH 5.5 and 7.4 [**a**, **b, c** were deduced from Ref. (Liu et al. 2008; Sun et al. 2008)]. **d** Non-covalent H-bonding of L-proline/GO hybrid (Tan et al. 2013a)

PEG (7 mg/kg, 200 μL), and NGO–PEG/DOX (10 mg/kg, 200 μL). The tumor region of NGO–PEG and NGO–PEG/DOX irradiated by NIR light (2 W/cm^2, 5 min) after 24 h of injection.

The time dependence of tumor volume is presented in Fig. 8b (the tumor volume normalized with respect to its initial size). Free DOX exposed rapid growth of tumor volume as a result of insufficient dosage to reduce it. NGO–PEG group showed reduction in the tumor volume after a few days of injection, and then follows its growth to reach the size of DOX group. NGO–PEG/DOX showed considerable trend with size reduction of tumor volume along a period of 30 days, this group demonstrated as a powerful vehicle for combined chemo-photothermal therapy of cancer in vivo. Figure 8c showed the weight loss of mice for the four groups as a function of time during the treatment. The result revealed that no weight loss was perceived, indicating that the toxicity of materials was not severed. On the other hand, Yang et al. reported for the first time the behavior of nanographene sheets in vivo by using PEG coating via a fluorescent labeling method, PEG-functionalized GO was labeled with the fluorescent dye Cy7 for in vivo investigations, the

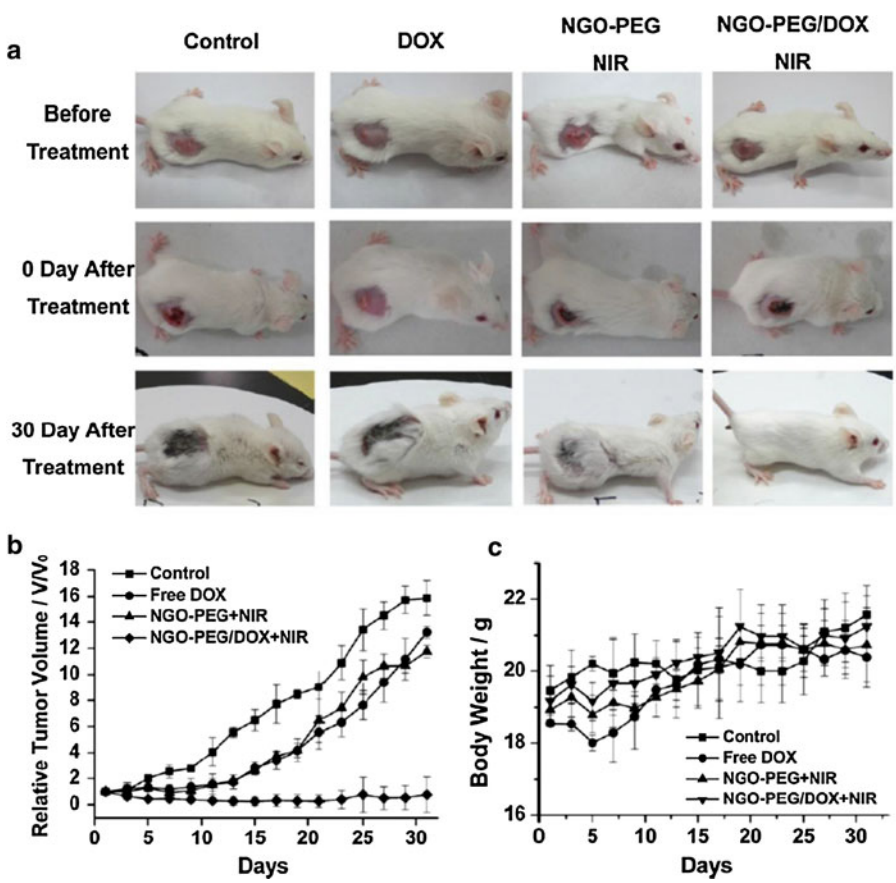

Fig. 8 **a** Photographs of mice groups after various treatments. **b** Tumor growth curves of different mice groups after treatment. **c** Body weights of mice groups after treatment. Deduced from Ref. (Zhang et al. 2011b)

majority of Cy7 dye molecules are covalently bonded to NGO–PEG via an amide bond formation. Three tumor models (4T1 tumor bearing Balb/c mice, KB, and U87MG tumor bearing nude mice) were demonstrated with different time points after intravenously injected by NGO–PEG–Cy7 (200 μL of 2 mg/mL solution for each mouse; a dose of 20 mg/kg) and subsequently imaged.

The concentration of NGO–PEG–Cy7 versus time was measured and the blood circulation half-life was observed approximately at 1.5 h (Fig. 9a). As shown in Fig. 9b, NGO–PEG–Cy7 existed in different tumor models over time, NGO–PEG exhibiting an excellent in vivo tumor near-infrared (NIR) photothermal therapy without obvious toxicity to the treated mice. Neither death nor noteworthy body weight drop was observed in the NGO–PEG plus laser-treated materials, as shown in c of Fig. 9. After 40 days of photothermal therapy, the major organs of treated mice were collected for histology analysis. The results exhibited no noticeable signal of organ distortion (Fig. 9d), suggesting the assure of using PEGylated NGS for in vivo applications (Yang et al. 2010). Table 2 summarizes the cytotoxicity and the cellular uptake in vitro and in vivo for various therapeutic systems.

Cytotoxicity of other carbon-based nanomaterials

Several studies emphasized that numerous factors such as chemical composition, size, shape, contaminants, concentration, and cell types will influence the cellular uptake and the cytotoxicity of carbon-based materials (Lam et al. 2004; Warheit et al. 2004; Sayes et al. 2005; Tsai et al. 2006; Schrand et al. 2007b; Liu et al. 2008; Casey et al. 2008; Shinohara et al. 2009; Yuan et al. 2010; Arlt et al. 2010; Zhang et al. 2010b; Chang et al. 2011; Liao et al. 2011; Yang et al. 2013; Chng and Pumera 2013). To the best of our knowledge, there are few experimental reports that compare the cytotoxicity of carbon nanomaterials (Schrand

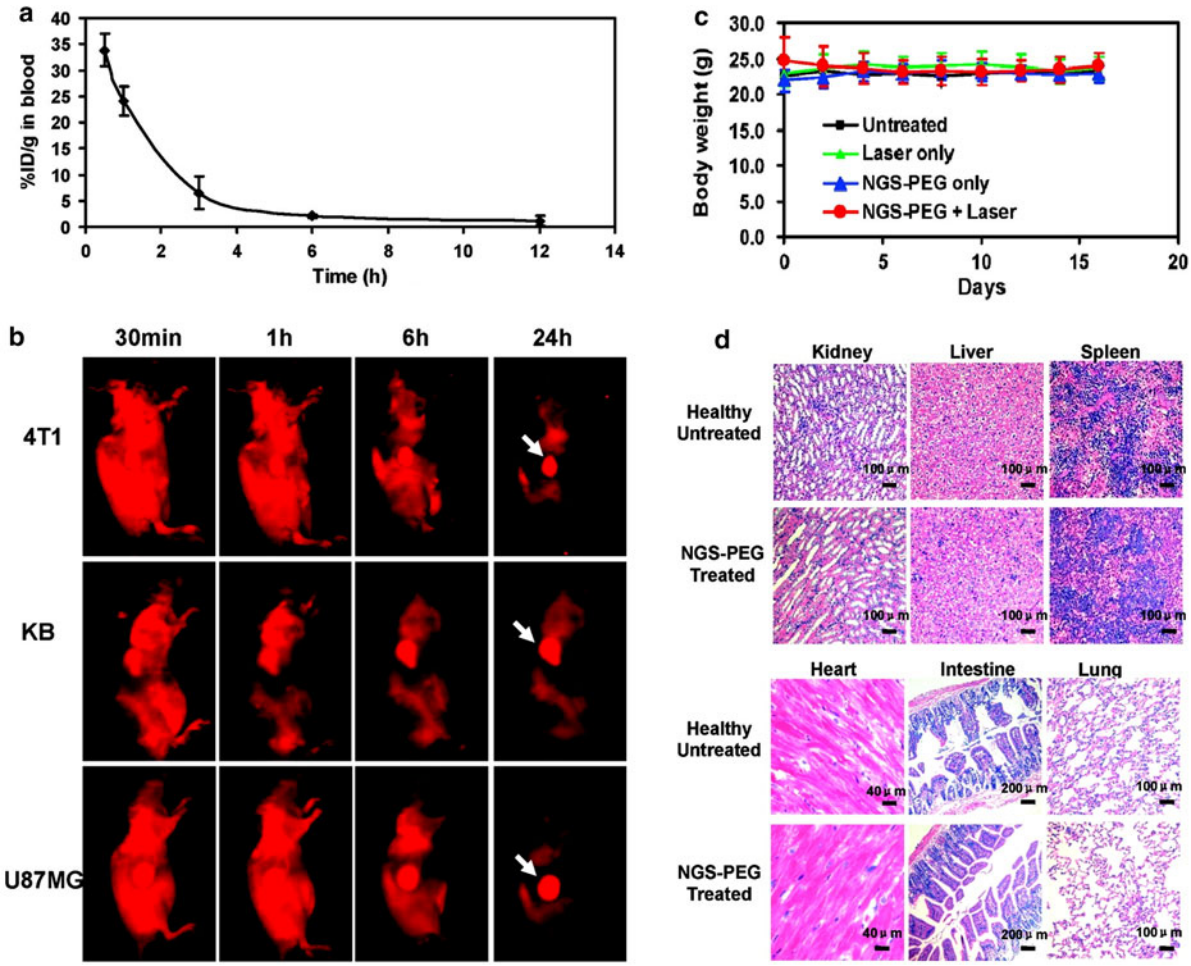

Fig. 9 **a** The blood circulation profile of NGS–PEG–Cy7 measured by Cy7 fluorescence in the blood at different time points post-injection. **b** In vivo fluorescence images of mice models at different time points post-injection of NGS–PEG–Cy7. Mouse autofluorescence was subtracted and high tumor uptake of NGS–PEG–Cy7 was observed for all the three tumor models. Hairs on Balb/c mice were removed before fluorescence imaging. **c** Body weight curves after diverse treatments. **d** H&E stained images of major organs. No noticeable change was observed in major organs including kidney, liver, spleen, heart, intestine, and lung [reproduced with permission from Ref. (Yang et al. 2010)]

et al. 2007a; Zhang et al. 2012). Table 3 highlights the cytotoxicity evaluation of carbon nanomaterials concerning the size, concentration, and biological systems. Compared with CNTs, PEGylated NGO exhibited distinctive in vivo behaviors such as reduced reticuloendothelial systems (RES) accumulation and particularly improved tumor passive targeting effect (Liu et al. 2007a). The unique 2D structure, small size (10–50 nm), and biocompatibility played an important role to enhance permeability and the retention effect of NGS for high tumor passive uptake. Compared with nanoparticles, such as gold nanorods (AuNRs) significantly explored as photothermal agents, the result showed that PEGylated NGS emerged as comparable with PEGylated AuNRs in terms of administration routes (intravenous), injected doses (20 mg/kg), NIR laser densities (2 W/cm^2), and irradiation durations (5 min) (von Maltzahn et al. 2009).

Fullerene is the first carbon nanomaterial investigated toward biomedical applications due to it being the first to be discovered, in 1985 (Krotto et al. 1985), and classified as an inorganic nanoparticle with wide availability due to its small size ($\sim$1 nm). Innate fullerene particles have very low dispersibility in water and form negative charge aggregates with an average size of 160 nm. Hence, OH groups and other

Table 2 In vitro and in vivo toxicity evaluation of therapeutic nanomaterial systems

Therapeutic systems	Concentration	Biological system	Results	References
GO-based therapeutic systems				
NGO–PEG–Rituxan/DOX	2, 10 μmol/L in terms of DOX	Raji and CEM cells	High selectivity at [DOX] = 10 μmol/L	Sun et al. (2008)
			Rituxan improved doxorubicin delivery into Raji B-cells	
			Less toxic than free DOX	
NGO–PEG/SN 38 loaded SN 38 showed	1 mg/mL in terms of SN38	HCT-116	High cancer cell killing potency in comparison with free SN38 molecules in organic solvents	Liu et al. (2008)
GO–pluronic (F38)/EA ellagic acid	100 wt% (GO–F38)	MCF7 and HT29	High drug loading capacity	Kakran et al. (2011)
			EA loaded onto the functionalized GO has less cytotoxicity than free EA	
GO–Tween 80 (T80)/EA	122 wt% (GO–T80)			
GO–maltodextrin (MD)/EA	114 wt% (GO–MD			
GO–CS–CPT	10 μM	HepG2	No obvious toxicity measured for GO–CS	Bao et al. (2011)
CS: chitosan		HeLa cells		
CPT: camptothecin			GO–CS/CPT possessed higher cytotoxic effect than free CPT	
GO–FA/Ce6	2:1 (wt/wt)	MGC 803	GO–FA is non-toxic	Huang et al. (2011)
	1:1 (wt/wt)		2:1 ratio revealed no dark toxicity	
	mGO–FA/mCe6		More than 80 % of cell viability	
			1:1 ratio revealed cell viability less than 50 %	
			Toxicity is concentration dependent	
NGS–PEG/125I	20 mg/kg	In vivo	PEGylated NGS largely gathered in the reticuloendothelial system	Yang et al. (2011a)
			No toxic effect at 20 mg/kg to the treated mice in a period of 3 months	
CNT-based therapeutic systems				
CNT–CP	20 wt% CNT–CP	DU145	No toxic effect observed for unloaded CNTs at 100 μg/mL	Arlt et al. (2010)
CNF–CP		PC-3		
	14 wt% of CNF–CP	A498		
		EJ28	No noteworthy toxicity observed for unloaded CNFs at 100 μg/mL	
			CNT–CP showed low cancer cell growth than free CP	
DOX–FA–CHI/ALG–SWCNT	300 wt%	HeLa cells	DOX–FA–CHI/ALG–SWCNTs are highly selective system and not cytotoxic	Zhang et al. (2009)
DOX–PL–PEG–SWCNT	~270 mg/L of DOX.	In vivo (SCID mice)	The SWCNT–DOX (5 mg/kg) exposed greater inhibition of tumor growth than free DOX	Liu et al. (2009)
			Mice treated with SWCNT–DOX possessed stable weight and no mortalities compared with free DOX	

Table 2 continued

Therapeutic systems	Concentration	Biological system	Results	References
Cisplatin–SWCNT	100 μg/mL	PC3	Free cisplatin and SWCNT–cisplatin have the same effect on PC3, but less effective DU145	Tripisciano et al. (2009)
		DU145		
C_{60}-based therapeutic systems				
C_{60}–PEI–FA/DTX	200 wt%	PC3	C_{60}–PEI–FA has no obvious toxicity to PC3	Shi et al. (2013)
DTX: docetaxel		In vivo: Murine S180	The system has higher inhibition efficiency than free DTX	
			C_{60}–PEI–FA/DTX is more effective than free DTX and C_{60}–PEI–FA in vivo	
Nano-C_{60} (water soluble)	0.24–2 ppb	HepG2	Nano-C_{60} has cytotoxic effect to tested cell lines after 48-h exposure	Sayes et al. (2005)
	400 ppb	HDF		
		NHA,		
$C_{60}(OH)_{24}$	100 μg/L	HDF and HepG2 cells	No cytotoxicity	Sayes et al. (2004)

organic molecules are induced in fullerene in order to activate its surface for better dispersibility in water and physiological media (Bosi et al. 2004; Han and Karim 2008) high dosages of fullerene particles, more than 70 mg/L lead to cell death after 24-h incubation, as the fullerene concentration and incubation time increases, the cell mortality increases (Han and Karim 2008). Numerous reports focused on in vitro and in vivo cellular uptake and toxicity evaluation of fullerene and its derivatives (Sayes et al. 2004, 2005; Bosi et al. 2004; Jia et al. 2005; Yamawaki and Iwai 2006; Porter et al. 2006; Han and Karim 2008; Kim et al. 2010; Cha et al. 2012). Jia et al. reported that unmodified C_{60} showed lower cytotoxicity than single- and multi-wall carbon nanotube to macrophages (Jia et al. 2005). The cellular uptake of human macrophages by C_{60} was very low, as low as that of treated SWCNTs, and their cytotoxicity was lower than that of graphite (Fiorito et al. 2006). Fullerene toxicity was evaluated in vivo on rats and fishes. Chem et al. demonstrated poly-alkylsulfonated C_{60} dispersion orally, intraperitoneally, and intravenously, the results revealed no lethal damage was observed by oral administration and the median lethal dose (LD_{50}) was approximated as 600 mg/kg in intraperitoneal administration. Nephropathy was induced after accumulation of materials in kidney by intraperitoneal and intravenous administration. The toxicological studies using fishes (Zhu et al. 2007; Usenko et al. 2008) showed C_{60} can act as a pro-oxidant and educe a toxic response via oxidative stress, considerable oxidative damage to brain lipids was reported and decrease in the hatching rate of zebra fish embryo and fin distortion. In summary, the toxicity parameters (shape, size, and oxygen species) of fullerene nanoparticles are still being evaluated. Major drawbacks are lipid peroxidation with functional groups mediating the toxicity and their accumulation in organs mainly in liver, due to massive binding with plasma protein and hindering their response for drug delivery applications. Furthermore, fullerene toxicity could be ascribed to their interaction with light (Prylutska et al. 2006), therefore, high controlled toxicity analysis of fullerene nanoparticles protected from light exposure, can evaluate the true toxic nature of fullerenes for medical applications. Carbon nanotubes in both forms, single- and multi-wall CNT, are widely considered to be as speculate materials for biomedical applications. The large length-to-diameter aspect ratio (more than 10^6;

Table 3 Toxicity evaluation of carbon nanomaterials

CNMs	Size	Concentration	Biological system	Results	References
GO	Below 200 nm	50 μg/mL	HeLa	No cytotoxic effect even at high concentration	Yang et al. (2011b)
GO	LD: 350 nm H: 3.9 nm LD: 2 μm H: 4.05	0–20 μg/mL	PMØ, J774A.1, LLC, MCF-7, HepG2, HUVEC, 48 h	No significant difference in cytotoxicity between 350 nm and 2 μm at different concentration	Yue et al. (2012)
GO	1,429.1 ± 89 nm H: 1.038 nm	20–100 μg/mL	HUVECs	Cell viability is concentration dependent	Cheng et al. (2013)
rGO	LD = 380 ± 0.4 μm LD = 11 ± 4 nm		hMSCs, 1 h	Cell destructions at 11 ± 4 nm 3.8 ± 0.4 mm has cytotoxic effect only at high concentration of 100 mg/mL time	Yue et al. (2012)
GO–CS	GO > 1,000 nm, 0.8–1.2 nm thickness GO–CS < 500 nm, 4–5 nm	1.0–100 mg/L (GO–CS)	HepG2 and HeLa cell lines	GO–CS has no obvious cytotoxicity, 80 % cell viability	Bao et al. (2011)
GO–PEG	5–50 nm	0.1–100 mg/L	HCT-116, 72 h	NGO–PEG exhibited no obvious toxicity	Liu et al. (2008)
SWCNTs	1 nm φ, 1 μmL	3.8 μg/mL	Mouse macrophage like cells	The macrophages consume high quantity of SWCNT without showing toxic effects	Cherukuri et al. (2004)
Functionalized SWCNTs	(1–5 nm φ, 0.1–1 μmL)	50 μg/mL	HL60, 3T3, CHO	No toxicity observed for SWCNTs and functionalized SWCNTs by endocytosis	Shi Kam et al. (2004)
SWCNTs, MWCNT and C_{60}	SWCNT (1.4 nm φ, 1 μmL) MWCNT (10–20 nm φ, 0.5–40 μmL	0–226 μg/cm^3	Guinea pig alveolar macrophage	SWCNTs cytotoxicity observed > 0.38 μg/cm^2 Cytotoxicity of MWCNTs was lower than SWCNTs	Jia et al. (2005)
SWCNTs, MWCNTs Carbon black (CB) Active carbon (AC)	SWCNT: 2 nm φ 500 nm L, sa: 3.15 μm^2) MWCNT: 50 nm φ 5 μmL, sa: 789 μm^2 CB: 200 nm (r) AC: 25 nm (r)	0–100 μg/cm^2	HDF: Human dermis fibroblasts cells	Cell survival rate: MWCNTs > CB > AC > SWCNTs	Tian et al. (2006)

Table 3 continued

CNMs	Size	Concentration	Biological system	Results	References
SWCNTs CB, SiO_2, ZnO	SWCNT: 8 nm φ, $L < 5$ μm CB, SiO_2, ZnO: 10–20 nm φ	5–100 μg/mL	PMEF:	SWCNTs revealed moderately cytotoxic effect than metal oxides, but persuaded more DNA damage	Yang et al. (2009b)
SWCNTs and MWCNTs	SWCNTs: 4 nm φ, 0.5–100 μm MWCNTs (15 nm φ, 0.5–200 μm)	200, 400 μ/mouse	In vivo (mouse)	SWCNTs are less toxic than MWCNTs	Nygaard et al. (2009)

1 mm length and 1 nm diameter) with high surface area makes it amenable for high molecular detection and recognition. Pristine CNTs are intrinsically insoluble in water and biological media, i.e., they cannot be explored directly in drug and bimolecular fields. Thus, CNTs should be functionalized to render them soluble and compatible in cell culture media. The toxicity of single- and multi-wall CNTs is attributed to numerous factors, for instance, length to diameter ratio, assay methods, functionalization, concentration, time of exposure, and nature of cells investigated. Wörle-Knirsch et al. found that the toxicity of SWCNTs depends on the preparation assay; the results showed that the viability of A549 decreased up to 40 % via MTT assay after addition of SWCNTs, but no changes on viability by using WST-1 assay method (Wörle-Knirsch et al. 2006).

Conclusion and perspectives

There is growing interest in GO as a material for biomedical application, in particular as a platform for drug delivery. This is due to the rich functional groups on the surface of the material which allow further facile functionalization to improve biocompatibility, dispersion, and of course drug loading. Within the review, the structure and properties of GO that allow covalent and non-covalent functionalization have been discussed. Toxicity investigations show functionalized GO to be biocompatible. Various works demonstrate GO derivatives are exciting nanocarriers for the loading and delivery of therapeutic drugs.

References

Acik M, Lee G, Mattevi C et al (2011) The role of oxygen during thermal reduction of graphene oxide studied by infrared absorption spectroscopy. J Phys Chem C 115:19761–19781. doi:10.1021/jp2052618

Agarwal S, Zhou X, Ye F et al (2010) Interfacing live cells with nanocarbon substrates. Langmuir 26:2244–2247. doi:10.1021/la9048743

Akhavan O (2010) The effect of heat treatment on formation of graphene thin films from graphene oxide nanosheets. Carbon 48:509–519. doi:10.1016/j.carbon.2009.09.069

Akhavan O, Ghaderi E (2010) Toxicity of graphene and graphene oxide nanowalls against bacteria. ACS Nano 4:5731–5736. doi:10.1021/nn101390x

Akhavan O, Ghaderi E, Akhavan A (2012) Size-dependent genotoxicity of graphene nanoplatelets in human stem cells. Biomaterials 33:8017–8025. doi:10.1016/j.biomaterials.2012.07.040

Altavilla C, Ciliberto E (2010) Inorganic nanoparticles: synthesis, applications, and perspectives. CRC Press, Taylor & Francis Group, Boca Raton

An J, Gou Y, Yang C et al (2013) Synthesis of a biocompatible gelatin functionalized graphene nanosheets and its application for drug delivery. Mater Sci Eng C. doi:10.1016/j.msec.2013.03.008

Arlt M, Haase D, Hampel S et al (2010) Delivery of carboplatin by carbon-based nanocontainers mediates increased cancer cell death. Nanotechnology 21:335101. doi:10.1088/0957-4484/21/33/335101

Bagri A, Mattevi C, Acik M et al (2010) Structural evolution during the reduction of chemically derived graphene oxide. Nat Chem 2:581–587. doi:10.1038/nchem.686

Bai H, Xu Y, Zhao L et al (2009) Non-covalent functionalization of graphene sheets by sulfonated polyaniline. Chem Commun 13:1667–1669. doi:10.1039/b821805f

Bao H, Pan Y, Ping Y et al (2011) Chitosan-functionalized graphene oxide as a nanocarrier for drug and gene delivery. Small 7:1569–1578. doi:10.1002/smll.201100191

Becerril HA, Mao J, Liu Z et al (2008) Evaluation of solution-processed reduced graphene oxide films as transparent conductors. ACS Nano 2:463–470. doi:10.1021/nn700375n

Bosi S, Feruglio L, Da Ros T et al (2004) Hemolytic effects of water-soluble fullerene derivatives. J Med Chem 47:6711–6715. doi:10.1021/jm0497489

Boukhvalov DW, Katsnelson MI (2008) Modeling of graphite oxide. J Am Chem Soc 130:10697–10701. doi:10.1021/ja8021686

Bourlinos AB, Gournis D, Petridis D et al (2003) Graphite oxide: chemical reduction to graphite and surface modification with primary aliphatic amines and amino acids. Langmuir 19:6050–6055. doi:10.1021/la026525h

Briggs D, Seah M (1990) Practical surface analysis. Wiley, Chichester

Brodie BC (1859) On the atomic weight of graphite. Philos Trans R Soc Lond 149:249–259. doi:10.1098/rstl.1859.0013

Buchsteiner A, Lerf A, Pieper J (2006) Water dynamics in graphite oxide investigated with neutron scattering. J Phys Chem B 110:22328–22338. doi:10.1021/jp0641132

Cai W, Piner RD, Stadermann FJ et al (2008) Synthesis and solid-state NMR structural characterization of 13C-labeled graphite oxide. Science 321:1815–1817. doi:10.1126/science.1162369

Cançado LG, Takai K, Enoki T et al (2008) Measuring the degree of stacking order in graphite by Raman spectroscopy. Carbon 46:272–275. doi:10.1016/j.carbon.2007.11.015

Casey A, Herzog E, Lyng FM et al (2008) Single walled carbon nanotubes induce indirect cytotoxicity by medium depletion in A549 lung cells. Toxicol Lett 179:78–84. doi:10.1016/j.toxlet.2008.04.006

Cha YJ, Lee J, Choi SS (2012) Apoptosis-mediated in vivo toxicity of hydroxylated fullerene nanoparticles in soil nematode *Caenorhabditis elegans*. Chemosphere 87:49–54. doi:10.1016/j.chemosphere.2011.11.054

Chang Y, Yang S-T, Liu J-H et al (2011) In vitro toxicity evaluation of graphene oxide on A549 cells. Toxicol Lett 200:201–210. doi:10.1016/j.toxlet.2010.11.016

Chen H, Müller MB, Gilmore KJ et al (2008) Mechanically strong, electrically conductive, and biocompatible graphene paper. Adv Mater 20:3557–3561. doi:10.1002/adma.200800757

Cheng C, Nie S, Li S et al (2013) Biopolymer functionalized reduced graphene oxide with enhanced biocompatibility via mussel inspired coatings/anchors. J Mater Chem B 1:265. doi:10.1039/c2tb00025c

Cherukuri P, Bachilo SM, Litovsky SH, Weisman RB (2004) Near-infrared fluorescence microscopy of single-walled carbon nanotubes in phagocytic cells. J Am Chem Soc 126:15638–15639. doi:10.1021/ja0466311

Chng ELK, Pumera M (2013) The toxicity of graphene oxides: dependence on the oxidative methods used. Chem Eur J 19:8227–8235. doi:10.1002/chem.201300824

Choi E-Y, Han TH, Hong J et al (2010) Noncovalent functionalization of graphene with end-functional polymers. J Mater Chem 20:1907. doi:10.1039/b919074k

Cote LJ, Kim F, Huang J (2009) Langmuir–Blodgett assembly of graphite oxide single layers. J Am Chem Soc 131:1043–1049. doi:10.1021/ja806262m

Das A, Chakraborty B, Sood AK (2008) Raman spectroscopy of graphene on different substrates and influence of defects. Bull Mater Sci 31:579–584. doi:10.1007/s12034-008-0090-5

Depan D, Shah J, Misra RDK (2011) Controlled release of drug from folate-decorated and graphene mediated drug delivery system: synthesis, loading efficiency, and drug release response. Mater Sci Eng C 31:1305–1312. doi:10.1016/j.msec.2011.04.010

Dideykin A, Aleksenskiy AE, Kirilenko D et al (2011) Monolayer graphene from graphite oxide. Diam Relat Mater 20:105–108. doi:10.1016/j.diamond.2010.10.007

Dresselhaus MS, Dresselhaus G, Saito R, Jorio A (2004) Raman spectroscopy of carbon nanotubes. Phys Rep 409:47–99. doi:10.1016/j.physrep.2004.10.006

Dreyer DR, Park S, Bielawski CW, Ruoff RS (2010) The chemistry of graphene oxide. Chem Soc Rev 39:228–240. doi:10.1039/b917103g

Du D, Wang L, Shao Y et al (2011) Functionalized graphene oxide as a nanocarrier in a multienzyme labeling amplification strategy for ultrasensitive electrochemical immunoassay of phosphorylated p53 (S392). Anal Chem 83:746–752. doi:10.1021/ac101715s

Duch MC, Budinger GRS, Liang YT et al (2011) Minimizing oxidation and stable nanoscale dispersion improves the biocompatibility of graphene in the lung. Nano Lett 11:5201–5207. doi:10.1021/nl202515a

Duong DL, Han GH, Lee SM et al (2012) Probing graphene grain boundaries with optical microscopy. Nature 490:235–239. doi:10.1038/nature11562

Eda G, Fanchini G, Chhowalla M (2008) Large-area ultrathin films of reduced graphene oxide as a transparent and flexible electronic material. Nat Nanotechnol 3:270–274. doi:10.1038/nnano.2008.83

Eda G, Mattevi C, Yamaguchi H et al (2009) Insulator to semimetal transition in graphene oxide. J Phys Chem C 113:15768–15771. doi:10.1021/jp9051402

Englert JM, Dotzer C, Yang G et al (2011) Covalent bulk functionalization of graphene. Nat Chem 3:279–286. doi:10.1038/NCHEM.1010

Fan X, Peng W, Li Y et al (2008) Deoxygenation of exfoliated graphite oxide under alkaline conditions: a green route to graphene preparation. Adv Mater 20:4490–4493. doi:10.1002/adma.200801306

Fan H, Wang L, Zhao K et al (2010) Fabrication, mechanical properties, and biocompatibility of graphene-reinforced chitosan composites. Biomacromolecules 11:2345–2351. doi:10.1021/bm100470q

Fang M, Wang K, Lu H et al (2009) Covalent polymer functionalization of graphene nanosheets and mechanical properties of composites. J Mater Chem 19:7098. doi:10.1039/b908220d

Feng L, Zhang S, Liu Z (2011) Graphene based gene transfection. Nanoscale 3:1252–1257. doi:10.1039/c0nr00680g

Ferrari AC, Robertson J (2004) Raman spectroscopy of amorphous, nanostructured, diamond-like carbon, and nanodiamond. Philos Trans Ser A Math Phys Eng Sci 362:2477–2512. doi:10.1098/rsta.2004.1452

Fiorito S, Serafino a, Andreola F, Bernier P (2006) Effects of fullerenes and single-wall carbon nanotubes on murine and human macrophages. Carbon 44:1100–1105. doi:10.1016/j.carbon.2005.11.009

Ganguly A, Sharma S, Papakonstantinou P, Hamilton J (2011) Probing the thermal deoxygenation of graphene oxide using high-resolution in situ X-ray-based spectroscopies. J Phys Chem C 115:17009–17019. doi:10.1021/jp203741y

Gilje S, Han S, Wang M et al (2007) A chemical route to graphene for device applications. Nano Lett 7:3394–3398. doi:10.1021/nl0717715

Gillies ER, Fréchet JMJ (2005) pH-responsive copolymer assemblies for controlled release of doxorubicin. Bioconjug Chem 16:361–368. doi:10.1021/bc049851c

Gómez-Navarro C, Weitz RT, Bittner AM et al (2007) Electronic transport properties of individual chemically reduced graphene oxide sheets. Nano Lett 7:3499–3503. doi:10.1021/nl072090c

Grimme S (2004) On the importance of electron correlation effects for the pi–pi interactions in cyclophanes. Chem Eur J 10:3423–3429. doi:10.1002/chem.200400091

Han B, Karim MN (2008) Cytotoxicity of aggregated fullerene C_{60} particles on CHO and MDCK cells. Scanning 30:213–220. doi:10.1002/sca.20081

Han P, Wang H, Liu Z et al (2011) Graphene oxide nanoplatelets as excellent electrochemical active materials for VO^{2+}/VO^{2+} and V^{2+}/V^{3+} redox couples for a vanadium redox flow battery. Carbon 49:693–700. doi:org/10.1016/j.carbon.2010.10.022

Haugstad G (2012) Atomic force microscopy: understanding basic modes and advanced applications. Wiely Inc., Hoboken

He H (1998) A new structural model for graphite oxide. Chem Phys Lett 287:53–56. doi:10.1016/S0009-2614(98)00144-4

He H, Riedl T, Lerf A, Klinowski J (1996) Solid-state NMR studies of the structure of graphite oxide. J Phys Chem 3654:19954–19958. doi:10.1021/jp961563t

Hirata M, Gotou T, Horiuchi S et al (2004) Thin-film particles of graphite oxide 1: high-yield synthesis and flexibility of the particles. Carbon 42:2929–2937. doi:10.1016/j.carbon.2004.07.003

Hofmann U, Holst R (2006) Über die Säurenatur und die Methylierung von Graphitoxyd. Ber Dtsch Chem Ges 72:754–771

Hu W, Peng C, Luo W et al (2010) Graphene-based antibacterial paper. ACS Nano 4:4317–4323. doi:10.1021/nn101097v

Hu W, Peng C, Lv M et al (2011) Protein corona-mediated mitigation of cytotoxicity of graphene oxide. ACS Nano 5:3693–3700. doi:10.1021/nn200021j

Hu H, Yu J, Li Y et al (2012) Engineering of a novel pluronic F127/graphene nanohybrid for pH responsive drug delivery. J Biomed Mater Res 100:141–148. doi:10.1002/jbm.a.33252

Huang P, Xu C, Lin J et al (2011) Folic acid-conjugated graphene oxide loaded with photosensitizers for targeting photodynamic therapy. Theranostics 1:240–250. doi:10.7150/thno/v01p0240

Hummers WS, Offeman RE (1958) Preparation of graphitic oxide. J Am Chem Soc 80:1339. doi:10.1021/ja01539a017

Jayakumar K, Rajesh R, Dharuman V et al (2012) Gold nano particle decorated graphene core first generation PAMAM dendrimer for label free electrochemical DNA hybridization sensing. Biosens Bioelectron 31:406–412. doi:10.1016/j.bios.2011.11.001

Jia G, Wang H, Yan L et al (2005) Cytotoxicity of carbon nanomaterials: single-wall nanotube, multi-wall nanotube, and fullerene. Environ Sci Technol 39:1378–1383. doi:10.1021/es048729l

Josepovits K, Sanakis Y, Petridis D, De I (2006) Evolution of surface functional groups in a series of progressively oxidized graphite oxides. Chem Mater 18:2740–2749. doi:10.1021/cm060258+

Jung I, Pelton M, Piner R et al (2007) Simple approach for high-contrast optical imaging and characterization of graphene-based sheets. Nano Lett 7:3569–3575. doi:10.1021/nl0714177

Jung I, Dikin D, Park S et al (2008a) Effect of water vapor on electrical properties of individual reduced graphene oxide sheets. J Phys Chem C 112:20264–20268. doi:10.1021/jp807525d

Jung I, Dikin DA, Piner RD, Ruoff RS (2008b) Tunable electrical conductivity of individual graphene oxide sheets reduced at "low" temperatures. Nano Lett 8:4283–4287. doi:10.1021/nl8019938

Jung I, Vaupel M, Pelton M et al (2008c) Characterization of thermally reduced graphene oxide by imaging ellipsometry. J Phys Chem C 112:8499–8506. doi:10.1021/jp802173m

Kakran M, Sahoo NG, Bao H et al (2011) Functionalized graphene oxide as nanocarrier for loading and delivery of ellagic acid. Curr Med Chem 18:4503–4512. doi:10.2174/092986711797287548

Kim KS, Zhao Y, Jang H et al (2009) Large-scale pattern growth of graphene films for stretchable transparent electrodes. Nature 457:706–710. doi:10.1038/nature07719

Kim K-T, Jang M-H, Kim J-Y, Kim SD (2010) Effect of preparation methods on toxicity of fullerene water suspensions to Japanese medaka embryos. Sci Total Environ 408:5606–5612. doi:10.1016/j.scitotenv.2010.07.055

Kim JM, Kim J, Kim J (2012) Covalent decoration of graphene oxide with dendrimer-encapsulated nanoparticles for universal attachment of multiple nanoparticles on chemically

converted graphene. Chem Commun 48:9233–9235. doi:10.1039/c2cc31780j
Kitano H, Tachimoto K, Anraku Y (2007) Functionalization of single-walled carbon nanotube by the covalent modification with polymer chains. J Colloid Interface Sci 306:28–33. doi:10.1016/j.jcis.2006.10.034
Kovtyukhova NI, Ollivier PJ, Martin BR et al (1999) Layer-by-layer assembly of ultrathin composite films from micron-sized graphite oxide sheets and polycations. Chem Mater 11:771–778. doi:10.1021/cm981085u
Krotto HW, Heath JR, O'Brien SC et al (1985) C_{60}: buckminsterfullerene. Nature 318:162–163. doi:10.1038/318162a0
Kudin KN, Ozbas B, Schniepp HC et al (2008) Raman spectra of graphite oxide and functionalized graphene sheets. Nano Lett 8:36–41. doi:10.1021/nl071822y
Kuila T, Bose S, Mishra AK et al (2012) Chemical functionalization of graphene and its applications. Prog Mater Sci 57:1061–1105. doi:10.1016/j.pmatsci.2012.03.002
Lahaye R, Jeong H, Park C, Lee Y (2009) Density functional theory study of graphite oxide for different oxidation levels. Phys Rev B Condens Matter 79:125435. doi:10.1103/PhysRevB.79.125435
Lam C-W, James JT, McCluskey R, Hunter RL (2004) Pulmonary toxicity of single-wall carbon nanotubes in mice 7 and 90 days after intratracheal instillation. Toxicol Sci 77:126–134. doi:10.1093/toxsci/kfg243
Larciprete R, Fabris S, Sun T et al (2011) Dual path mechanism in the thermal reduction of graphene oxide. J Am Chem Soc 133:17315–17321. doi:10.1021/ja205168x
Layek RK, Samanta S, Chatterjee DP, Nandi AK (2010) Physical and mechanical properties of poly(methyl methacrylate) -functionalized graphene/poly(vinylidine fluoride) nanocomposites: piezoelectric β polymorph formation. Polymer 51:5846–5856. doi:10.1016/j.polymer.2010.09.067
Lee EC, Kim D, Jurecka P et al (2007) Understanding of assembly phenomena by aromatic–aromatic interactions: benzene dimer and the substituted systems. J Phys Chem A 111:3446–3457. doi:10.1021/jp068635t
Lee V, Whittaker L, Jaye C et al (2009) Large-area chemically modified graphene films: electrophoretic deposition and characterization by Soft X-ray absorption spectroscopy. Chem Mater 21:3905–3916. doi:10.1021/cm901554p
Lee DY, Khatun Z, Lee J-H et al (2011) Blood compatible graphene/heparin conjugate through noncovalent chemistry. Biomacromolecules 12:336–341. doi:10.1021/bm101031a
Lerf A, He H, Forster M, Klinowski J (1998) Structure of graphite oxide revisited. J Phys Chem B 102 :4477–4482. doi:10.1021/jp9731821
Liao K-H, Lin Y-S, Macosko CW, Haynes CL (2011) Cytotoxicity of graphene oxide and graphene in human erythrocytes and skin fibroblasts. ACS Appl Mater Interfaces 3:2607–2615. doi:10.1021/am200428v
Lin Y, Jin J, Song M (2011) Preparation and characterisation of covalent polymer functionalized graphene oxide. J Mater Chem 21:3455. doi:10.1039/c0jm01859g
Liu Z, Cai W, He L et al (2007a) In vivo biodistribution and highly efficient tumour targeting of carbon nanotubes in mice. Nat Nanotechnol 2:47–52. doi:10.1038/nnano.2006.170
Liu Z, Sun X, Nakayama-Ratchford N, Dai H (2007b) Supramolecular chemistry on water-soluble carbon nanotubes for drug loading and delivery. ACS Nano 1:50–56. doi:10.1021/nn700040t
Liu Z, Robinson JT, Sun X, Dai H (2008) PEGylated nanographene oxide for delivery of water insoluble cancer drugs. J Am Chem Soc 130:10876–10877. doi:10.1021/ja803688x
Liu Z, Fan AC, Rakhra K et al (2009) Supramolecular stacking of doxorubicin on carbon nanotubes for in vivo cancer therapy. Angew Chem Int Ed 48:7668–7672. doi:10.1002/anie.200902612
Liu Y, Yu D, Zeng C et al (2010) Biocompatible graphene oxide-based glucose biosensors. Langmuir 26:6158–6160. doi:10.1021/la100886x
Liu K, Zhang J–J, Cheng F–F et al (2011) Green and facile synthesis of highly biocompatible graphene nanosheets and its application for cellular imaging and drug delivery. J Mater Chem 21:12034. doi:10.1039/c1jm10749f
Liu Z, Wang Y, Zhang N (2012) Micelle-like nanoassemblies based on polymer-drug conjugates as an emerging platform for drug delivery. Expert Opin Drug Deliv 9:805–822. doi:10.1517/17425247.2012.689284
Loh KP, Bao Q, Ang PK, Yang J (2010a) The chemistry of graphene. J Mater Chem 20:2277. doi:10.1039/b920539j
Loh KP, Bao Q, Eda G, Chhowalla M (2010b) Graphene oxide as a chemically tunable platform for optical applications. Nat Chem 2:1015–1024. doi:10.1038/nchem.907
Lomeda JR, Doyle CD, Kosynkin DV et al (2008) Diazonium functionalization of surfactant-wrapped chemically converted graphene sheets. J Am Chem Soc 130:16201–16206. doi:10.1021/ja806499w
Lu C-H, Yang H–H, Zhu C-L et al (2009) A graphene platform for sensing biomolecules. Angew Chem Int Ed 48:4785–4787. doi:10.1002/anie.200901479
Lu N, Yin D, Li Z, Yang J (2011) Structure of graphene oxide: thermodynamics versus Kinetics. J Phys Chem C 115:11991–11995. doi:10.1021/jp204476q
Ma JC, Dougherty DA (2012) The cation–π interaction. Chem Rev 97:1303–1324. doi:10.1021/ar300265y
Makharza S, Cirillo G, Bachmatiuk A et al (2013) Size-dependent nanographene oxide as a platform for efficient carboplatin release. J Mater Chem B. doi:10.1039/b000000x
Malard LM, Pimenta MA, Dresselhaus G, Dresselhaus MS (2009) Raman spectroscopy in graphene. Phys Rep 473:51–87. doi:10.1016/j.physrep.2009.02.003
Marcano DC, Kosynkin DV, Berlin JM et al (2010) Improved synthesis of graphene oxide. ACS Nano 4:4806–4814. doi:10.1021/nn1006368
Marcus P, Maurice V (2006) Passivation of metals and semiconductors, and properties of thin oxide layers: a selection of papers from the 9th international symposium, Paris, France, 27 June–1 July 2005, first edit., p 764
Marques PAAP, Gonçalves G, Cruz S et al (2011) Functionalized graphene nanocomposites. In: Hashim A (ed) Advances in nanocomposite technology. InTech, Rijeka, p 347
Mattevi C, Eda G, Agnoli S et al (2009) Evolution of electrical, chemical, and structural properties of transparent and conducting chemically derived graphene thin films. Adv Funct Mater 19:2577–2583. doi:10.1002/adfm.200900166
Moazzami Gudarzi M (2012) Enhancement of dispersion and bonding of graphene–polymer through wet transfer of

functionalized graphene oxide. eXPRESS Polym Lett 6:1017–1031. doi:10.3144/expresspolymlett.2012.107

Mohanty N, Berry V (2008) Graphene-based single-bacterium resolution biodevice and DNA transistor: interfacing graphene derivatives with nanoscale and microscale biocomponents. Nano Lett 8:4469–4476. doi:10.1021/nl802412n

Murakami T, Ajima K, Miyawaki J et al (2004) Drug-loaded carbon nanohorns: adsorption and release of dexamethasone in vitro. Mol Pharm 1:399–405. doi:10.1021/mp049928e

Nair RR, Blake P, Grigorenko AN et al (2008) Fine structure constant defines visual transparency of graphene. Science 320:1308. doi:10.1126/science.1156965

Novoselov KS, Geim AK, Morozov SV et al (2004) Electric field effect in atomically thin carbon films. Science 306:666–669. doi:10.1126/science.1102896

Novoselov KS, Jiang D, Schedin F et al (2005) Two-dimensional atomic crystals. Proc Natl Acad Sci USA 102:10451–10453. doi:10.1073/pnas.0502848102

Nygaard UC, Hansen JS, Samuelsen M et al (2009) Single-walled and multi-walled carbon nanotubes promote allergic immune responses in mice. Toxicol Sci 109:113–123. doi:10.1093/toxsci/kfp057

Paci JT, Belytschko T, Schatz GC (2007) Computational studies of the structure, behavior upon heating, and mechanical properties of graphite oxide. J Phys Chem C 111:18099–18111. doi:10.1021/jp075799g

Paredes JI, Villar-Rodil S, Martínez-Alonso A, Tascón JMD (2008) Graphene oxide dispersions in organic solvents. Langmuir 24:10560–10564. doi:10.1021/la801744a

Paredes JI, Villar-Rodil S, Solís-Fernández P et al (2009) Atomic force and scanning tunneling microscopy imaging of graphene nanosheets derived from graphite oxide. Langmuir 25:5957–5968. doi:10.1021/la804216z

Park S, Ruoff RS (2009) Chemical methods for the production of graphenes. Nat Nanotechnol 4:217–224. doi:10.1038/nnano.2009.58

Park S, Mohanty N, Suk JW et al (2010) Biocompatible, robust free-standing paper composed of a TWEEN/graphene composite. Adv Mater 22:1736–1740. doi:10.1002/adma.200903611

Pasricha R, Gupta S, Srivastava AK (2009) A facile and novel synthesis of Ag-graphene-based nanocomposites. Small 5:2253–2259. doi:10.1002/smll.200900726

Pimenta MA, Dresselhaus G, Dresselhaus MS et al (2007) Studying disorder in graphite-based systems by Raman spectroscopy. Phys Chem Chem Phys 9:1276–1291. doi:10.1039/b613962k

Porter AE, Muller K, Skepper J et al (2006) Uptake of C_{60} by human monocyte macrophages, its localization and implications for toxicity: studied by high resolution electron microscopy and electron tomography. Acta Biomater 2:409–419. doi:10.1016/j.actbio.2006.02.006

Prylutska SV, Burlaka AP, Matyshevska OP et al (2006) Effect of the visible light irradiation of fullerene-containing composites on the ROS generation and the viability of tumor cells. Exp Oncol 28:160–162

Qin XC, Guo ZY, Liu ZM et al (2012) Folic acid-conjugated graphene oxide for cancer targeted chemo-photothermal therapy. J Photochem Photobiol B Biol 120:156–162. doi:10.1016/j.jphotobiol.2012.12.005

Reich S, Thomsen C (2004) Raman spectroscopy of graphite. Philos Trans Ser A Math Phys Eng Sci 362:2271–2288. doi:10.1098/rsta.2004.1454

Riley KE, Pitonák M, Jurecka P, Hobza P (2010) Stabilization and structure calculations for noncovalent interactions in extended molecular systems based on wave function and density functional theories. Chem Rev 110:5023–5063. doi:10.1021/cr1000173

Rousseau DL, Bauman RP, Porto SPS (1981) Normal mode determination in crystals. J Raman Spectrosc 10:253–290. doi:10.1002/jrs.1250100152

Ruess G (1946) Über das Graphitoxyhydroxyd (Graphitoxyd). Monatsh Chem 76:381–417

Salavagione HJ, Gómez MA, Martínez G (2009) Polymeric modification of graphene through esterification of graphite oxide and poly(vinyl alcohol). Macromolecules 42:6331–6334. doi:10.1021/ma900845w

Salvio R, Krabbenborg S, Naber WJM et al (2009) The formation of large-area conducting graphene-like platelets. Chem Eur J 15:8235–8240. doi:10.1002/chem.200900661

Sayes CM, Fortner JD, Guo W et al (2004) The differential cytotoxicity of water-soluble fullerenes. Nano Lett 4:1881–1887. doi:10.1021/nl0489586

Sayes CM, Gobin AM, Ausman KD et al (2005) Nano-C_{60} cytotoxicity is due to lipid peroxidation. Biomaterials 26:7587–7595. doi:10.1016/j.biomaterials.2005.05.027

Schniepp HC, Li J-L, McAllister MJ et al (2006) Functionalized single graphene sheets derived from splitting graphite oxide. J Phys Chem B 110:8535–8539. doi:10.1021/jp060936f

Scholz W, Boehm HP (2004) Untersuchungen am Graphitoxid. VI. Betrachtungen Betrachtungen zur struktur des graphitoxids. Z Anorg Allg Chem 369:327–340. doi:10.1002/zaac.19693690322

Schrand AM, Dai L, Schlager JJ et al (2007a) Differential biocompatibility of carbon nanotubes and nanodiamonds. Diam Relat Mater 16:2118–2123. doi:10.1016/j.diamond.2007.07.020

Schrand AM, Huang H, Carlson C et al (2007b) Are diamond nanoparticles cytotoxic? J Phys Chem B 111:2–7. doi:10.1021/jp066387v

Shen J, Hu Y, Shi M et al (2009) Fast and facile preparation of graphene oxide and reduced graphene oxide nanoplatelets. Chem Mater 21:3514–3520. doi:10.1021/cm901247t

Shen H, Liu M, He H et al (2012) PEGylated graphene oxide-mediated protein delivery for cell function regulation. ACS Appl Mater Interfaces 4:6317–6323. doi:10.1021/am3019367

Shi Kam NW, Jessop TC, Wender PA, Dai H (2004) Nanotube molecular transporters: internalization of carbon nanotube-protein conjugates into Mammalian cells. J Am Chem Soc 126:6850–6851. doi:10.1021/ja0486059

Shi J, Zhang H, Wang L et al (2013) PEI-derivatized fullerene drug delivery using folate as a homing device targeting to tumor. Biomaterials 34:251–261. doi:10.1016/j.biomaterials.2012.09.039

Shin H-J, Kim KK, Benayad A et al (2009) Efficient reduction of graphite oxide by sodium borohydride and its effect on electrical conductance. Adv Funct Mater 19:1987–1992. doi:10.1002/adfm.200900167

Shinohara N, Matsumoto K, Endoh S et al (2009) In vitro and in vivo genotoxicity tests on fullerene C_{60} nanoparticles.

Toxicol Lett 191:289–296. doi:10.1016/j.toxlet.2009.09.012

Si Y, Samulski ET (2008) Synthesis of water soluble graphene. Nano Lett 8:1679–1682. doi:10.1021/nl080604h

Singh NJ, Min SK, Kim DY, Kim KS (2009) Comprehensive energy analysis for various types of π-interaction. J Chem Theory Comput 5:515–529. doi:10.1021/ct800471b

Stankovich S, Piner RD, Nguyen ST, Ruoff RS (2006) Synthesis and exfoliation of isocyanate-treated graphene oxide nanoplatelets. Carbon 44:3342–3347. doi:10.1016/j.carbon.2006.06.004

Stankovich S, Dikin Da, Piner RD et al (2007) Synthesis of graphene-based nanosheets via chemical reduction of exfoliated graphite oxide. Carbon 45:1558–1565. doi:10.1016/j.carbon.2007.02.034

Staudenmaier L (1898) Verfahren zur Darstellung der Graphitslure. Ber Dtsch Chem Ges 31:1481–1487. doi:10.1002/cber.18980310237

Sun X, Liu Z, Welsher K et al (2008) Nano-graphene oxide for cellular imaging and drug delivery. Nano Res 1:203–212. doi:10.1007/s12274-008-8021-8

Sun X, Luo D, Liu J, Evans DG (2010) Monodisperse chemically modified graphene obtained by density gradient ultracentrifugal rate separation. ACS Nano 4:3381–3389. doi:10.1021/nn1000386

Szűts A, Szabó-Révész P (2012) Sucrose esters as natural surfactants in drug delivery systems—a mini-review. Int J Pharm 433:1–9. doi:10.1016/j.ijpharm.2012.04.076

Takahashi K, Yamada K, Kato H et al (2012) In situ scanning electron microscopy of graphene growth on polycrystalline Ni substrate. Surf Sci 606:728–732. doi:10.1016/j.susc.2011.12.009

Tan R, Li C, Luo J et al (2013a) An effective heterogeneous L-proline catalyst for the direct asymmetric aldol reaction using graphene oxide as support. J Catal 298:138–147. doi:10.1016/j.jcat.2012.11.024

Tan X, Feng L, Zhang J et al (2013b) Functionalization of graphene oxide generates a unique interface for selective serum protein interactions. ACS Appl Mater Interfaces 5:1370–1377. doi:10.1021/am302706g

Tang S, Cao Z (2012) Site-dependent catalytic activity of graphene oxides towards oxidative dehydrogenation of propane. Phys Chem Chem Phys 14:16558–16565. doi:10.1039/c2cp41343d

Tarakeshwar P, Choi HS, Kim KS (2001) Olefinic vs. aromatic pi-H interaction: a theoretical investigation of the nature of interaction of first-row hydrides with ethene and benzene. J Am Chem Soc 123:3323–3331. doi:10.1021/ja0013531

Tian F, Cui D, Schwarz H et al (2006) Cytotoxicity of single-wall carbon nanotubes on human fibroblasts. Toxicol In Vitro 20:1202–1212. doi:10.1016/j.tiv.2006.03.008

Titelman GI, Gelman V, Bron S et al (2005) Characteristics and microstructure of aqueous colloidal dispersions of graphite oxide. Carbon 43:641–649. doi:10.1016/j.carbon.2004.10.035

Tripisciano C, Kraemer K, Taylor A, Borowiak-Palen E (2009) Single-wall carbon nanotubes based anticancer drug delivery system. Chem Phys Lett 478:200–205. doi:10.1016/j.cplett.2009.07.071

Tsai S-F, Yang C, Liu B-L et al (2006) Role of oxidative stress in thuringiensin-induced pulmonary toxicity. Toxicol Appl Pharmacol 216:347–353. doi:10.1016/j.taap.2006.05.013

Usenko CY, Harper SL, Tanguay RL (2008) Fullerene C_{60} exposure elicits an oxidative stress response in embryonic zebrafish. Toxicol Appl Pharmacol 229:44–55. doi:10.1016/j.taap.2007.12.030

Vashist SK, Zheng D, Pastorin G et al (2011) Delivery of drugs and biomolecules using carbon nanotubes. Carbon 49:4077–4097. doi:10.1016/j.carbon.2011.05.049

Veca LM, Lu F, Meziani MJ et al (2009) Polymer functionalization and solubilization of carbon nanosheets. Chem Commun 18:2565–2567. doi:10.1039/b900590k

Vickerman JC (1997) Surface analysis—the principal techniques. Wiley, Chichester

Von Maltzahn G, Park J-H, Agrawal A et al (2009) Computationally guided photothermal tumor therapy using long-circulating gold nanorod antennas. Cancer Res 69:3892–3900. doi:10.1158/0008-5472.CAN-08-4242

Wang S, Chia P-J, Chua L–L et al (2008) Band-like transport in surface-functionalized highly solution-processable graphene nanosheets. Adv Mater 20:3440–3446. doi:10.1002/adma.200800279

Wang K, Ruan J, Song H et al (2010a) Biocompatibility of graphene oxide. Nanoscale Res Lett 6:8. doi:10.1007/s11671-010-9751-6

Wang L, Sun YY, Lee K et al (2010b) Stability of graphene oxide phases from first-principles calculations. Phys Rev B Condens Matter 82:161406. doi:10.1103/PhysRevB.82.161406

Wang C, Lv P, Wei W et al (2011) A smart multifunctional nanocomposite for intracellular targeted drug delivery and self-release. Nanotechnology 22:415101. doi:10.1088/0957-4484/22/41/415101

Wang XW, Zhang C, Wang PL et al (2012) Enhanced performance of biodegradable poly(butylene succinate)/graphene oxide nanocomposites via in situ polymerization. Langmuir 28:7091–7095. doi:10.1021/la204894h

Warheit DB, Laurence BR, Reed KL et al (2004) Comparative pulmonary toxicity assessment of single-wall carbon nanotubes in rats. Toxicol Sci 77:117–125. doi:10.1093/toxsci/kfg228

Warner JH, Schaffel F, Bachmatiuk A, Rummeli M (2012) Graphene: fundamentals and emergent applications. Elsever Inc., Oxford

Wate PS, Banerjee SS, Jalota-Badhwar A et al (2012) Cellular imaging using biocompatible dendrimer-functionalized graphene oxide-based fluorescent probe anchored with magnetic nanoparticles. Nanotechnology 23:415101. doi:10.1088/0957-4484/23/41/415101

Widenkvist E (2010) Fabrication and functionalization of graphene and other carbon nanomaterials in solution. Uppsala University, Uppsala

Wilson NR, Pandey PA, Beanland R et al (2009) Graphene oxide: structural analysis and application as a highly transparent support for electron microscopy. ACS Nano 3:2547–2556. doi:10.1021/nn900694t

Wood JD, Schmucker SW, Lyons AS et al (2011) Effects of polycrystalline Cu substrate on graphene growth by chemical vapor deposition. Nano Lett 11:4547–4554. doi:10.1021/nl201566c

Wörle-Knirsch JM, Pulskamp K, Krug HF (2006) Oops they did it again! Carbon nanotubes hoax scientists in viability assays. Nano Lett 6:1261–1268. doi:10.1021/nl060177c

Xiao Z, Chen W (2012) Cell biocompatibility of functionalized graphene oxide. Acta Phys Chim Sin 28:1520–1524. doi:10.3866/PKU.WHXB201203131

Xu Y, Liu Z, Zhang X et al (2009) A Graphene hybrid material covalently functionalized with porphyrin: synthesis and optical limiting property. Adv Mater 21:1275–1279. doi:10.1002/adma.200801617

Xue Y, Liu Y, Lu F et al (2012) Functionalization of graphene oxide with oolyhedral oligomeric silsesquioxane (POSS) for multifunctional applications. J Phys Chem Lett 3: 1607–1612. doi:10.1021/jz3005877

Yamawaki H, Iwai N (2006) Cytotoxicity of water-soluble fullerene in vascular endothelial cells. Am J Physiol Cell Physiol 290:C1495–C1502. doi:10.1152/ajpcell.0.0481.2005

Yan J-A, Chou MY (2010) Oxidation functional groups on graphene: structural and electronic properties. Phys Rev B Condens Matter 82:125403. doi:10.1103/PhysRevB.82.125403

Yan L, Zhao F, Li S et al (2011) Low-toxic and safe nanomaterials by surface-chemical design, carbon nanotubes, fullerenes, metallofullerenes, and graphenes. Nanoscale 3:362–382. doi:10.1039/c0nr00647e

Yang D, Velamakanni A, Bozoklu G et al (2009a) Chemical analysis of graphene oxide films after heat and chemical treatments by X-ray photoelectron and Micro-Raman spectroscopy. Carbon 47:145–152. doi:10.1016/j.carbon.2008.09.045

Yang H, Liu C, Yang D et al (2009b) Comparative study of cytotoxicity, oxidative stress and genotoxicity induced by four typical nanomaterials: the role of particle size, shape and composition. J Appl Toxicol 29:69–78. doi:10.1002/jat.1385

Yang H, Shan C, Li F et al (2009c) Covalent functionalization of polydisperse chemically-converted graphene sheets with amine-terminated ionic liquid. Chem Commun 26: 3880–3882. doi:10.1039/b905085j

Yang K, Zhang S, Zhang G et al (2010) Graphene in mice: ultrahigh in vivo tumor uptake and efficient photothermal therapy. Nano Lett 10:3318–3323. doi:10.1021/nl100996u

Yang K, Wan J, Zhang S et al (2011a) In vivo pharmacokinetics, long-term biodistribution, and toxicology of PEGylated graphene in mice. ACS Nano 5:516–522. doi:10.1021/nn1024303

Yang X, Wang Y, Huang X et al (2011b) Multi-functionalized graphene oxide based anticancer drug-carrier with dual-targeting function and pH-sensitivity. J Mater Chem 21:3448–3454. doi:10.1039/c0jm02494e

Yang K, Hu L, Ma X et al (2012a) Multimodal imaging guided photothermal therapy using functionalized graphene nanosheets anchored with magnetic nanoparticles. Adv Mater 24:1868–1872. doi:10.1002/adma.201104964

Yang K, Wan J, Zhang S et al (2012b) The influence of surface chemistry and size of nanoscale graphene oxide on photothermal therapy of cancer using ultra-low laser power. Biomaterials 33:2206–2214. doi:10.1016/j.biomaterials.2011.11.064

Yang Q, Pan X, Clarke K, Li K (2012c) Covalent functionalization of graphene with polysaccharides. Ind Eng Chem Res 51:310–317. doi:10.1021/ie201391e

Yang K, Li Y, Tan X et al (2013) Behavior and toxicity of graphene and its functionalized derivatives in biological systems. Small 9:1492–1503. doi:10.1002/smll.201201417

Yi H-B, Diefenbach M, Choi YC et al (2006) Interactions of neutral and cationic transition metals with the redox system of hydroquinone and quinone: theoretical characterization of the binding topologies, and implications for the formation of nanomaterials. Chem Eur J 12:4885–4892. doi:10.1002/chem.200501551

Yi H-B, Lee HM, Kim KS (2009) Interaction of benzene with transition metal cations: theoretical study of structures, energies, and IR spectra. J Chem Theory Comput 5: 1709–1717. doi:10.1021/ct900154x

Yuan Y, Wang X, Jia G et al (2010) Pulmonary toxicity and translocation of nanodiamonds in mice. Diam Relat Mater 19:291–299. doi:10.1016/j.diamond.2009.11.022

Yuan Q, Hu H, Gao J et al (2011) Upright standing graphene formation on substrates. J Am Chem Soc 133: 16072–16079. doi:10.1021/ja2037854

Yue H, Wei W, Yue Z et al (2012) The role of the lateral dimension of graphene oxide in the regulation of cellular responses. Biomaterials 33:4013–4021. doi:10.1016/j.biomaterials.2012.02.021

Zhang T-Y, Zhang D (2011) Aqueous colloids of graphene oxide nanosheets by exfoliation of graphite oxide without ultrasonication. Bull Mater Sci 34:25–28. doi:10.1007/s12034-011-0048-x

Zhang X, Meng L, Lu Q et al (2009) Targeted delivery and controlled release of doxorubicin to cancer cells using modified single wall carbon nanotubes. Biomaterials 30:6041–6047. doi:10.1016/j.biomaterials.2009.07.025

Zhang L, Xia J, Zhao Q et al (2010a) Functional graphene oxide as a nanocarrier for controlled loading and targeted delivery of mixed anticancer drugs. Small 6:537–544. doi:10.1002/smll.200901680

Zhang X, Yin J, Kang C et al (2010b) Biodistribution and toxicity of nanodiamonds in mice after intratracheal instillation. Toxicol Lett 198:237–243. doi:10.1016/j.toxlet.2010.07.001

Zhang Y, Ali SF, Dervishi E et al (2010c) Cytotoxicity effects of graphene and single-wall carbon nanotubes in neural phaeochromocytoma-derived PC12 cells. ACS Nano 4:3181–3186. doi:10.1021/nn1007176

Zhang S, Yang K, Feng L, Liu Z (2011a) In vitro and in vivo behaviors of dextran functionalized graphene. Carbon 49:4040–4049. doi:10.1016/j.carbon.2011.05.056

Zhang W, Guo Z, Huang D et al (2011b) Synergistic effect of chemo-photothermal therapy using PEGylated graphene oxide. Biomaterials 32:8555–8561. doi:10.1016/j.biomaterials.2011.07.071

Zhang X, Yin J, Peng C et al (2011c) Distribution and biocompatibility studies of graphene oxide in mice after intravenous administration. Carbon 49:986–995. doi:10.1016/j.carbon.2010.11.005

Zhang X, Hu W, Li J et al (2012) A comparative study of cellular uptake and cytotoxicity of multi-walled carbon nanotubes, graphene oxide, and nanodiamond. Toxicol Res 1:62. doi:10.1039/c2tx20006f

Zhao J, Pei S, Ren W et al (2010) Efficient preparation of large-area graphene oxide sheets for transparent conductive films. ACS Nano 4:5245–5252. doi:10.1021/nn1015506

Zhong Q, Inniss D, Kjoller K, Elings VB (1993) Fractured polymer/silica fiber surface studied by tapping mode atomic force microscopy. Surf Sci 290:L688–L692. doi:10.1016/0039-6028(93)90582-5

Zhong X, Jin J, Li S et al (2010) Aryne cycloaddition: highly efficient chemical modification of graphene. Chem Commun 46:7340–7342. doi:10.1039/c0cc02389b

Zhu X, Zhu L, Li Y et al (2007) Developmental toxicity in zebrafish (*Danio rerio*) embryos after exposure to manufactured nanomaterials: buckminsterfullerene aggregates (nC_{60}) and fullerol. Environ Toxicol Chem 26:976–979. doi:10.1897/06-583.1